

FOR REFERENCE
NOT TO BE TAKEN FROM THIS ROOM

RECEIVED
MAY 17 01
ELECTRICAL ENGINEERING

SPEED CONTROL OF
INDUCTION MOTORS
BY POWER TRANSISTORS

by

Necdet ÇARDAK

Bogazici University Library

39001100316283 14

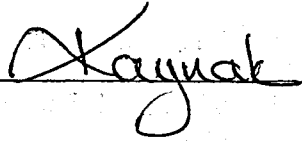
Submitted to the Faculty of the
School of Engineering in Partial Fulfillment
of the Requirements for the Degree of
MASTER OF SCIENCE
in
ELECTRICAL ENGINEERING

Bogaziçi University

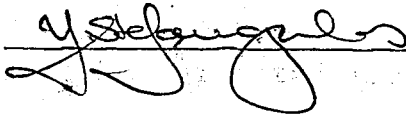
April 1981

This Thesis has been approved:

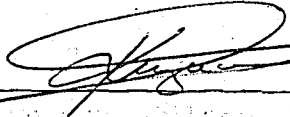
Dr. Okyay KAYNAK
(Thesis Supervisor)



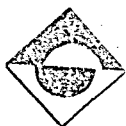
Dr. Yorgo ISTEфанOPULOS



Dr. Ahmet KUZUCU



Date: April 1981



ACKNOWLEDGEMENT

This thesis has been prepared for the partial fulfillment of the requirements of Bogazici University, School of Engineering for the degree of Master of Science in Electrical Engineering.

The author wishes to express his gratitude and sincere thanks to Dr. Okyay KAYNAK, thesis supervisor, for his kind interest and guidance in the accomplishment of this work. Thanks are also given to Gülsen Karşıt, who typed the manuscript.

ABSTRACT

In this thesis, the speed control of a 3-phase induction motor by electronic circuitry is investigated and compared with alternative methods used in industry.

The design of the control unit to synthesise a 3-phase stepped waveform and the following power amplifiers is described and the experimental results are compared with the theoretical values.

ÖZET

Bu tez çalışmasında elektronik devreler vasıtasıyla denetlenen 3 fazlı asenkron motor hız kontrolü incelenmiş ve uygulamada kullanılan diğer yöntemlerle karşılaştırılmıştır.

Denetleyicinin tasarımı, uygulanması ve denemesi yapılarak kuramsal ve deneysel sonuçlar verilmiştir. Ayrıca deneysel neticelerle teorik neticeler karşılaştırılmıştır.

TABLE OF CONTENTS

ACKNOWLEDGEMENTS

ABSTRACT

ÖZET

INTRODUCTION	1
CHAPTER 1 - INDUCTION MOTOR CONTROL	4
1.1 Types of A.C. Motors	4
1.2 Rotating Fields	6
1.3 Speeds of A.C. Motors	8
1.4 Electronic Speed Control Systems	12
CHAPTER 2 - POWER TRANSISTORS IN VARIABLE SPEED DRIVES	27
2.1 Power Transistors in Speed Control Systems	27
2.2 A Unijunction Transistor Pulse Generator Circuit and Wave Shaper	36
2.3 3Ø Logic	40
2.4 3Ø Logic Delay	43
2.5 Darlington Output	44
CHAPTER 3 - A.C. MOTOR OPERATION WITH NON-SINUSOIDAL SUPPLY WAVEFORMS AND VARIABLE-FREQUENCY OPERATION OF INDUCTION MOTOR	51
3.1 Harmonic Behavior of A.C. Motors	51
3.2 Steady-State Performance at Constant Volts/Hz	65

CHAPTER 4 - EXPERIMENTAL RESULTS AND CONCLUSIONS	72
4.1 Experimental Results	72
4.2 Conclusions and Suggestions	76
4.3 Closed Loop Operation	77
REFERENCES	80
APPENDIX 1 - Measurements of the Components V.C.O.	81
APPENDIX 2 - Truth Tables of J-K and D Type Flip-Flop	82
APPENDIX 3 - Equivalent Circuit of the Polyphase Induction Motor	83
APPENDIX 4 - Fourier Analysis of Non-Sinusoidal Waveform	88
APPENDIX 5 - Cost Evaluation	94
APPENDIX 6 - Complete Diagram of the System	95

INTRODUCTION

The three-phase induction motor is probably the most important prime mover for integral-horsepower industrial applications. For the same weight, the rating of a single-phase induction motor is only about 60% that of the poly-phase machine. Both efficiency and power factor are lower in single-phase motors. However, the three-phase induction motor has often exasperated the application of speed control and can only be provided by the wound-rotor types, but the range is not competitive with that available from dc motors. "If only we could vary the applied frequency," was a remark often made in the era before solid state. Of course, in some implementations, the frequency was made variable by the use of another motor/alternator set. Such strategy is obviously not economical.

The design of an adjustable-frequency, three-phase supply is not difficult if a compromise is made with regard to wave-shape. Although a square wave would result in high eddy-current and hysteresis losses, it is still not necessary to synthesize a true sine wave. A stepped waveform consisting of six segments can be created by mixing logic pulses. Such a waveform will have relatively

low third-harmonic energy- the chief culprit in eddy-current and hysteresis dissipation. The use of digital logic provides great simplification because IC modules displace complex discrete circuits in all three phases.

Another aspect of variable-frequency control is the necessity of changing the motor voltage by the same percentage as the frequency change. If voltage and frequency change by the same amount, then, there will be no change in no-load current or motor flux. In small motors, this basic requirement can be circumvented by inserting resistances in each motor lead. However, such a technique would not be allowable with large motors unless the speed variation were restricted. The use of such resistance also degrades the speed regulation of the motor.

In this thesis, the design, the construction of a speed control circuitry is described in which consideration is given to the points mentioned in the above paragraphs.

The three-phase wave synthesis imparted by the digital logic modules commences with a pulse train. Six power channels provide the required sequence of voltage steps needed to develop the quasi-sine wave. This sequence is repeated at 120 degree intervals in order to supply three phase energy to the motor. Harmonic analysis

of the resulting waveform is carried out and it is shown that there exists no even harmonics, neither do the third and multiples of the third harmonics. The current and voltage waveforms are obtained and it is seen that as the goes up, current waveform approaches to a sine wave.

When the d.c. supply is adjusted for 220 volts, the motor receives three-phase power at 50 Hz. With 20 volts from dc supply, the three-phase power supplied to the motor has a frequency of 5 Hz. The speed range corresponding to such a voltage reduction is approximately 1420 rpm to 142 rpm, for four poles induction motor.

Due to the voltage rating of the transistor used (80V) speed control could be checked only between 5 Hz and 18 Hz. Below 5 Hz, the starting torque was not sufficient as is explained in the thesis. Within the quoted range very smooth control of speed was possible. If the power output transistors are replaced by higher voltage rated ones, the set will be suitable for speed control of up to 10 HP motors in 1:10 speed range.

The thesis concludes with remarks on further possible work for closed loop operation.

CHAPTER 1

INDUCTION MOTOR CONTROL

Direct current motors are widely used for the application of adjustable speed drives in industry. But it still has its age-old commutator arcing and maintenance problems. The dc motor is also expensive and the failure rate is more than the induction motor. These advantages make the induction motor more attractive for the controllable source of mechanical rotating power in industry.

1.1. TYPES OF A.C. MOTORS

In general, torque and the resulting rotation or linear motion in electric motors results from interaction of two magnetic fields. One of these fields may be provided by a permanent magnet but more often both are produced by electric currents. The nature of the current supplied to electric motors and the manner in which their windings and magnetic structures are arranged give rise to a wide variety of designs. Of all electric motors manufactured for industry the three-phase induction motor

with a cage rotor has for three-quarters of a century been the type which, for one or more of the following reasons, has been produced in the greatest numbers.

(a) Since the majority of motors are required to produce steady rotation and the rotating magnetic field eliminates many of the design problems associated with providing continuous torque, the polyphase-induction motor is eminently suitable for approximately constant speed application. Only small modifications can make it synchronous, which on public electricity supplies means absolutely constant speed over its full operating range.

(b) Three-phase alternating current supplies have been adopted universally for distribution of electrical energy, and there is a considerable measure of standardization. In such supplies the three phases peak sequentially in time at intervals equal to one-third of the system periodicity. By arranging the three-phase windings around the airgap so that the poles generated are also in space-sequence, a rotating field is set up.

(c) The rotor draws power by transformer action from the stationary windings distributed in the stator slots and converts it into mechanical power.

(d) The absence of brushes makes it possible to operate induction motors with cage or solid rotors under

very adverse conditions and ensure considerable reliability.

1.2. ROTATING FIELDS

Figure 1.1 shows how a symmetrical three-phase winding when supplied from a balanced three-phase power supply produces a rotating field. Each phase is represented by two turns spanning one pole pitch of a two-pole motor. The arrow shows the direction of the current in phase A at the instant when it has maximum positive value. In the phasor diagram it is represented by I_A , I_B and I_C are the other two phase currents at 120 degree intervals. If the phasor diagram is now imagined to rotate in an anticlockwise direction at supply frequency the variation of current or field magnitude with time may be considered. One complete rotation or one cycle is completed in $1/f$ seconds, so that for a 50 Hz alternating current the 30 degree steps occur at one six-hundredth second intervals. If the instantaneous value of each phase current is now shown in its correct spatial position under the developed windings it can be seen that the m.m.f produced by the stator is also sinusoidally distributed. Successive diagrams show the field distribution at the above-mentioned time intervals and illustrate how the field wave travels across the winding face, which in a cylindrical airgap means rotation. In the synchronous two-pole motor the

$$i = \hat{I} \sin \omega t$$

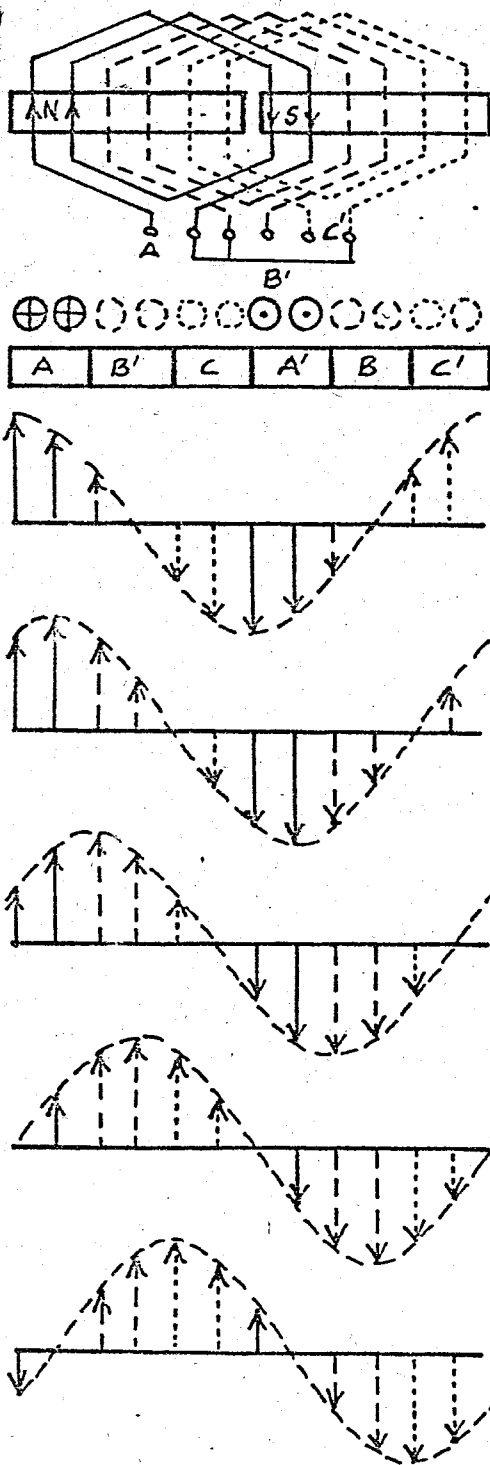
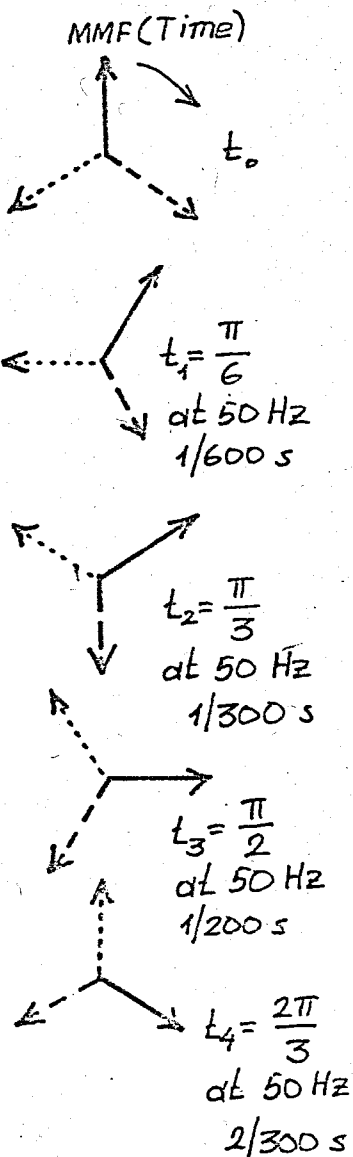


FIGURE 1.1. Symmetrical Three-Phase Winding Supplied from a Balanced Three-Phase Power Supply.

rotor will have turned through 120 mechanical degrees or one-third of a revolution. The synchronous speed of two-pole induction motors is, therefore, f rev/s or $60f$ rev/min. If a motor is now wound to produce p pole pairs the m.m.f. wave will now move only $1/p$ degrees and the synchronous speed becomes

$$N_s = \frac{60f}{p} \text{ rev/min} \quad (1.1)$$

For 50 Hz motors 4, 6, 8 and 10 pole synchronous speeds are therefore 1500, 1000, 750 and 600 rev/min respectively.

1.3. SPEEDS OF A.C. MOTORS

The speed of an induction motor is

$$n = n_s(1-s) \quad (1.2)$$

where n_s is the synchronous speed, and, s is the slip at that speed. The synchronous speed, n_s , is (from 1.1)

$$n_s = \frac{60f}{p}$$

where

f - supply frequency

p - number of pole pairs

Equations (1.1) and (1.2) gives speed control. Speed control is achieved by slip control. The slip in the motor is given by
$$n = \frac{60f}{p} (1-s) \quad (1.3)$$

Equation (1.3) shows that the speed of an induction motor can be controlled by:

1. increasing slip
2. changing the number of poles
3. varying supply frequency and voltage

The speed control method of induction motors are based upon these possibilities.

There are two kinds of induction motors. One is the squirrel-cage and the other is the wound-rotor. In the former the rotor circuit is short circuited, and in the latter there are 3 slip-rings on the same shaft which are connected to the rotor circuit.

Special design of cage rotors can match motor and load characteristics and so reduce the size of the motor required. More torque per ampere of starting current can also save on control equipment and generally increase the flexibility of the drive.

If the cage is replaced by a winding brought out to collector-(slip-) rings the rotor resistance can be varied externally and provides not only improved starting

characteristics but a measure of speed control. Such control is achieved by dissipating power as heat in the external resistances so that this method can prove not only inconvenient but costly for large powers. Special auxiliary machines which can convert power at slip frequency and return it to the supply are now superseded by commutator motors and electronic controllers which are able to provide a wide range of continuously variable speeds.

Speed control of the induction motor by changing the number of poles is generally applied to the squirrel-cage type. For this type of control the stator winding has to be designed so that by simple changes in coil connections the number of poles can be changed in the ratio 2 to 1. Either of two synchronous speeds can be selected. If a wound rotor is used additional complications are introduced because the rotor winding also must be rearranged for pole changing.

The synchronous speed of an induction motor is directly proportional to the applied frequency. Speed control of induction motor is obtained by supplying the stator electrical power from an adjustable-frequency solid-state inverter or using a wound-rotor induction motor as a frequency changer. The induction motor will follow the frequency within the slip frequency. Such a

control method is efficient and can be made highly accurate.

In some applications such as grinding spindles, portable tools, and woodworking machinery high speeds are required or the weight must be as small as possible. To achieve a high power-to-weight ratio the speed must be increased substantially which, for induction motors, means higher frequencies such as 250 and 400 Hz which, in the case of two-pole windings, gives synchronous speeds of 15000 and 24000 rev/min respectively.

For aircraft and military applications mainly 400 Hz motors are used and these may be useful in industry where their cost and the provision of a suitable frequency changer for groups of motors can be economically justified.

The speed of induction motors can be controlled electronically either by controlling the power input (varying the firing angle of the thyristors), or by connecting them to inverters, or cycloconverters (frequency changers).

1.4. ELECTRONIC SPEED CONTROL SYSTEMS

The speed control of induction motor can be achieved either by power transistors or by thyristors, or by triacs.

(a) SINGLE PHASE SWITCHING: The method of speed control for any polyphase machine is based here on the idea of rotating an alternating field in a machine, as opposed to rotating a field which is constant in amplitude. A variety of circuits and switching systems can be devised to achieve this. Such a realization is described in Reference 2, in which a 3-phase winding is fed from a single-phase supply, rotation of the magnetic field being ensured by sequential switching of the triacs. This is shown in Figure 1.2a.

The single-phase supply is, in effect rotated around the 3-phase winding by the switching elements 1 to 6. Either of the two supply terminals, x and y, can be connected to any one or more of the winding terminals A, B and C. The switching sequence listed in Table 1 gives 6-step anticlockwise rotation of the single-phase supply around the stator winding.

It is clear that this method of switching produces a result which is similar to the anticlockwise rotation

of a single winding fed from a single-phase supply as shown in Figure 1.2b. The normal forward (clockwise) rotation of the rotor in any conventional machine which is capable of single-phase operation will be reduced in speed according to the switching rate w_m . If the switching sequence is reversed, there will be a corresponding increase in the forward speed of the rotor.

TABLE 1
6-Step Switching Sequence for the Triac
Bridge System Shown in Figure 1

A	C	B	T1	T2	T3	T4	T5	T6
x		y	1	0	0	0	0	1
	x	y	0	0	1	0	0	1
y	x		0	1	1	0	0	0
y		x	0	1	0	0	1	0
	y	x	0	0	0	1	1	0
x	y		1	0	0	1	0	0

If the single-phase a.c. supply in Figure 1.2 is replaced by a d.c. supply, and if the switching elements were thyristors, normal d.c. link inverter operation is obtained. The rotating field is then substantially constant in amplitude. The important practical difference is that, whereas the d.c. supply has to be forcibly switched off between steps, the single phase a.c. supply can be allowed to switch off naturally at current zeros. The

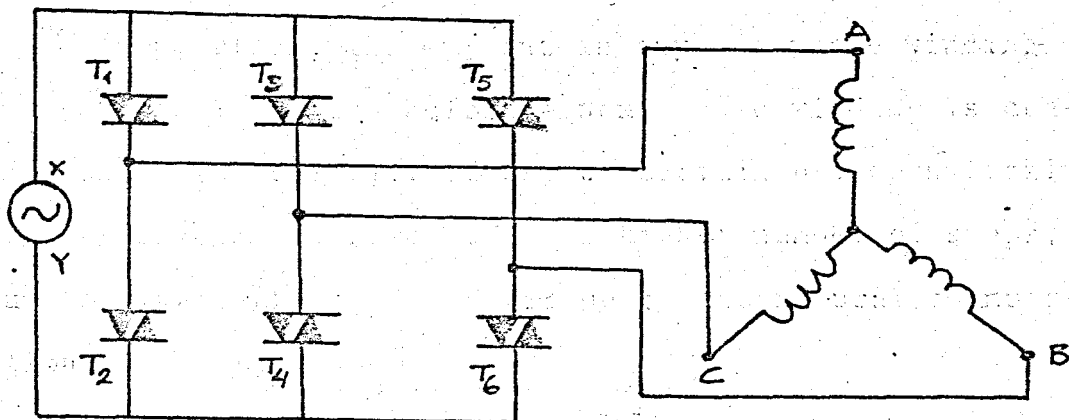


FIGURE 1.2a. 3-Phase Winding Fed From a Single-Phase Supply.

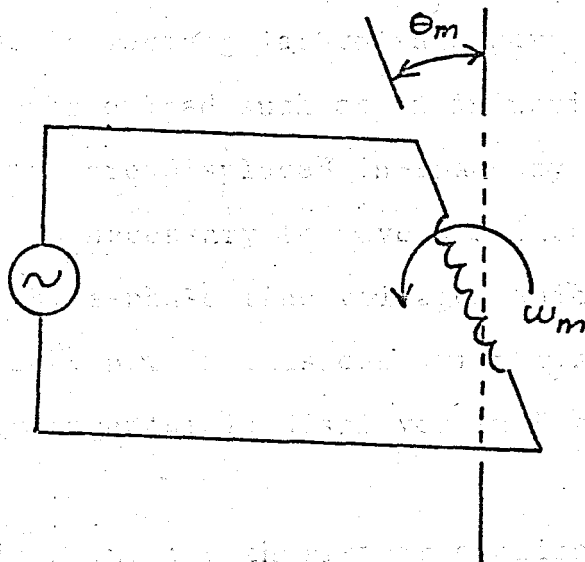


FIGURE 1.2b. Anticlockwise Rotation of a Single Winding Fed From a Single-Phase Supply.

switching elements have to be capable of conducting in either direction, and, therefore, as solid-state devices these have to be triacs, as shown in Figure 1.2a, or inverse parallel thyristors.

In practice, the current in any one phase winding may not fall to zero before a next phase winding is connected in the circuit. Thus, at certain 6-step switching is, in effect, transformed to a higher number of steps, up to a maximum of 12, by virtue of the natural commutation of the system.

(b) THREE-PHASE INDUCTION MOTOR CONTROL BY THYRISTOR:

Ideally the thyristor is a switch. It is on or it is off. If the supply were direct current and neglecting C and L switching transients, a thyristor in the line would produce a rectangular voltage wave across the load. For a three-phase load such as an induction motor, whose three windings are displaced in space by 120 electrical degrees, it is necessary to have a switching configuration to produce three-phase line voltages which are also displaced by 120° , but in this case with respect to time. The basic arrangement is displayed in Figure 1.4.

By triggering the thyristors cyclically without or with varying degrees of overlap a quasi three-phase supply is produced. The winding voltages with the triggering pulses are indicated in Figure 1.5 for no voltage overlap.

Figure 1.6 illustrates the behavior of the mmf pattern in the air-gap of the motor as a function of time. Over interval 0 to 1 (in Figure 1.5) current flows in

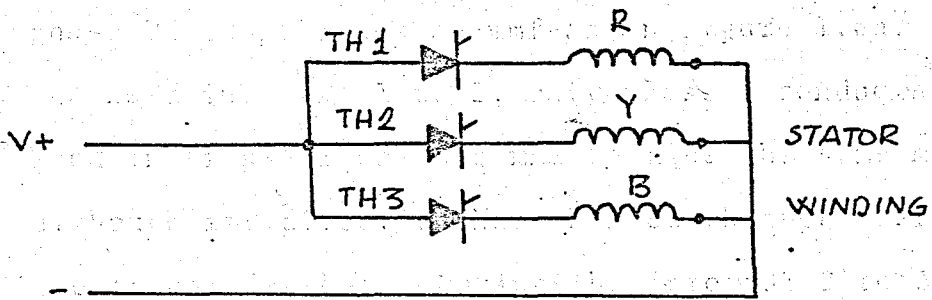


FIGURE 1.4. Half Wave Bridge Inverter.

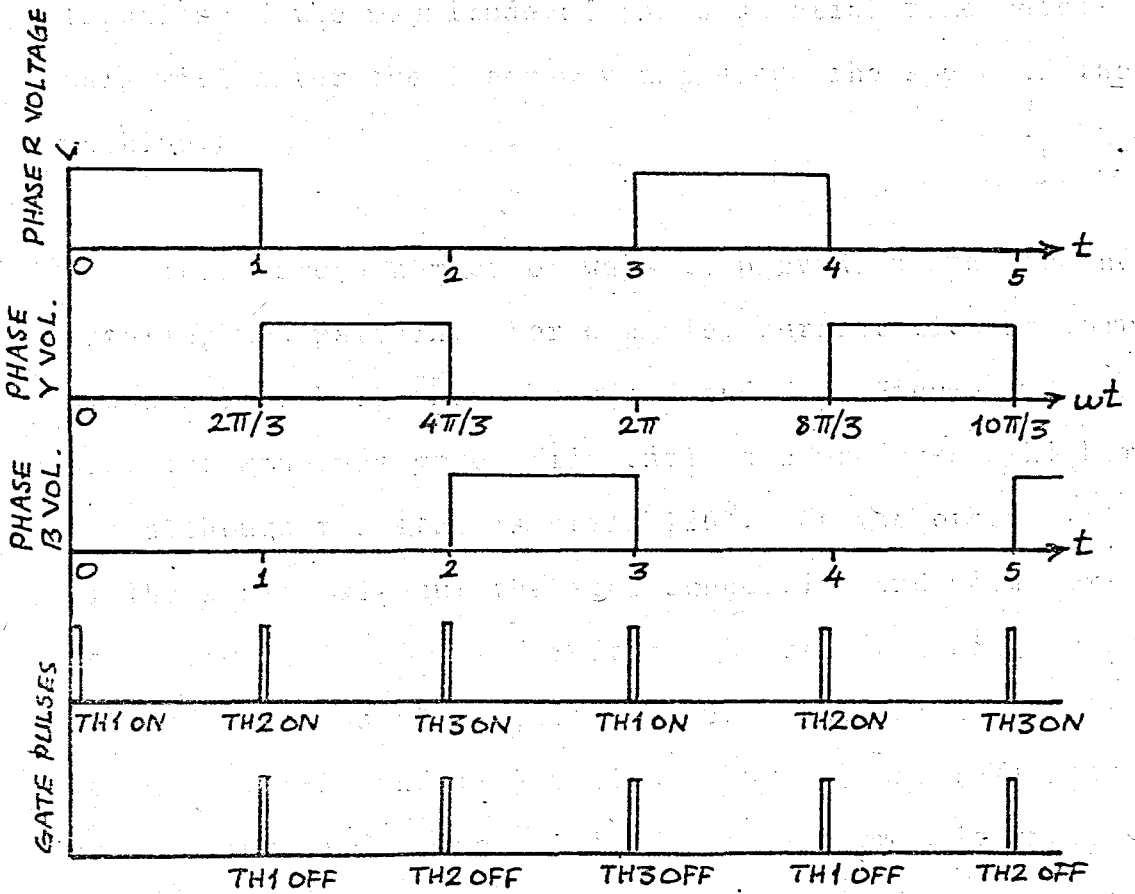


FIGURE 1.5. Load Voltage Waveform and Triggering Sequence.

phase R and produces an mmf as in Figure 1.6a. During the next interval 1 to 2, only phase Y conducts and as seen in Figure 1.6b, the mmf retains the same magnitude although its direction has changed through a step of 120 electrical degrees. During the interval 2 to 3 the mmf changes through another 120° until interval 3 to 4 when it is back to its original direction having rotated through 360 electrical degrees and completed a cycle. This stepping mmf produces a quasi rotating magnetic flux which is required for the induction motor operation. Alteration of the magnitude of the sequential time intervals will alter the frequency and hence the speed of the machine.

There are a number of ways to provide a stepped and rotating mmf pattern. For example, current flowing through R and B together, then through B and Y of Figure 1.4 uses the windings more efficiently and produces a higher mmf although the step is still 120°. At the other end of the scale, without the star connection and with current flowing in either direction through each winding a 30° step is possible. This entails a switching arrangement (+R), (-B) and (-Y) followed by (+R) and (-Y), etc. as in Figure 1.7. The magnitudes of the mmf alternate with each 30° step so there is imbalance. For the most efficient use of the windings and following as close as possible to a sinusoidal supply, a full three phase

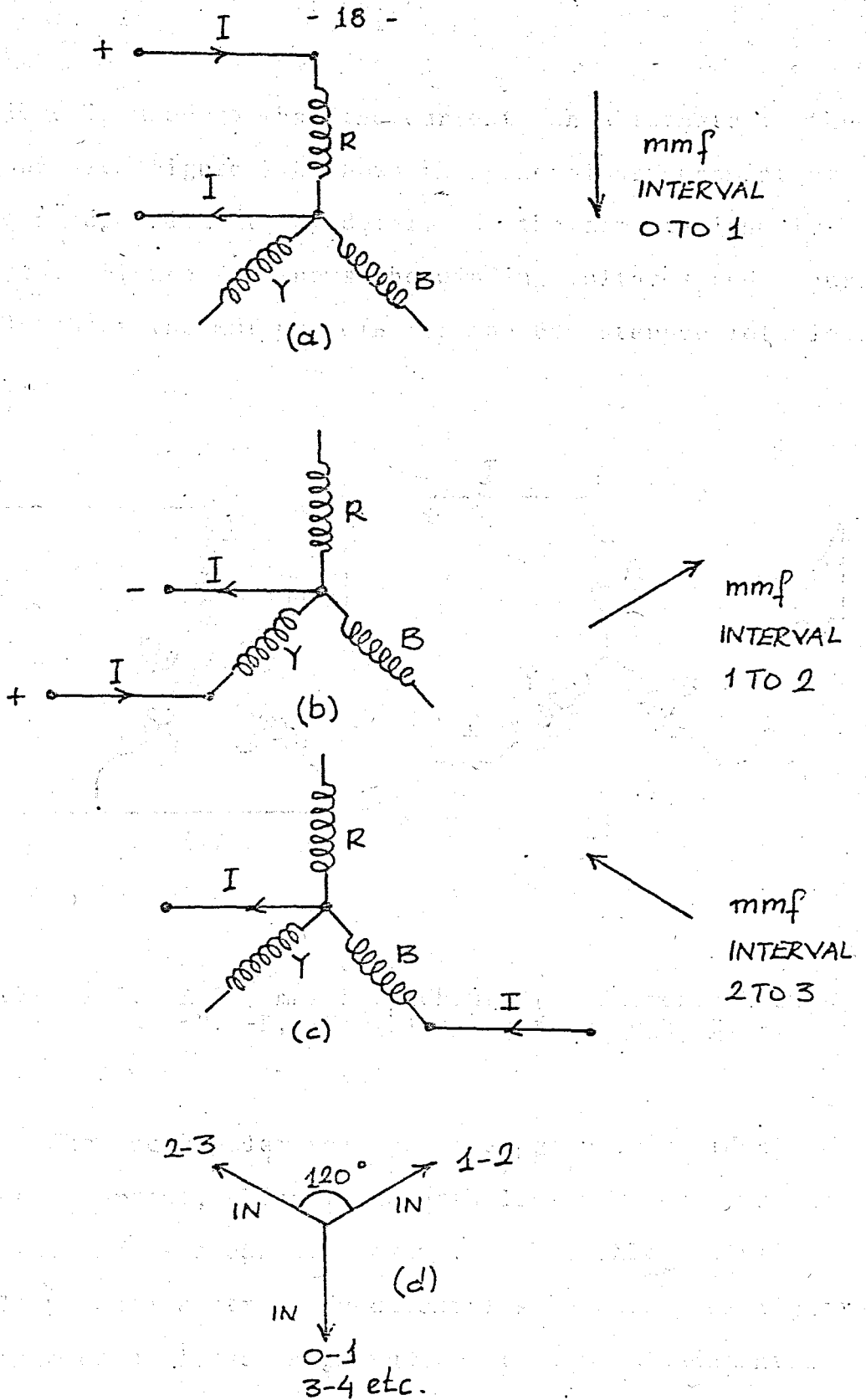


FIGURE 1.6. Mmf Pattern. (a) mmf interval 0 to 1; (b) mmf interval 1 to 2; (c) mmf interval 2 to 3; (d) mmf phase relation for each interval.

bridge is used so that the current can alternate in the windings. Figure 1.8 shows the general arrangement at the bridge without any details of the commutation circuits. Figure 1.9 shows the winding voltages and Figure 1.10 shows the mmf pattern for the 60° stepped rotation.

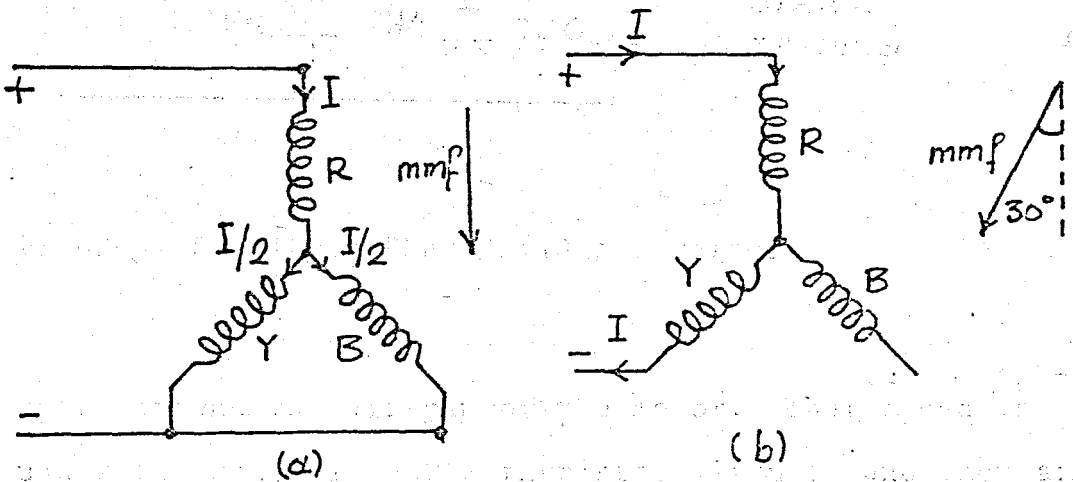


FIGURE 1.7. A 30° mmf Step Change (a) Current through +R, -B, -Y; (b) current through +R, -Y.

The rectangular voltage wave produces an ideal steady current, which is nevertheless bidirectional and so the mmf is stepped. However, a harmonic analysis will produce a strong fundamental sine wave plus higher harmonics of lesser magnitude. It is the fundamental wave whose energy does useful work and the higher create losses. Neglecting the higher harmonics the fundamental wave will produce the mmf which rotates at this constant

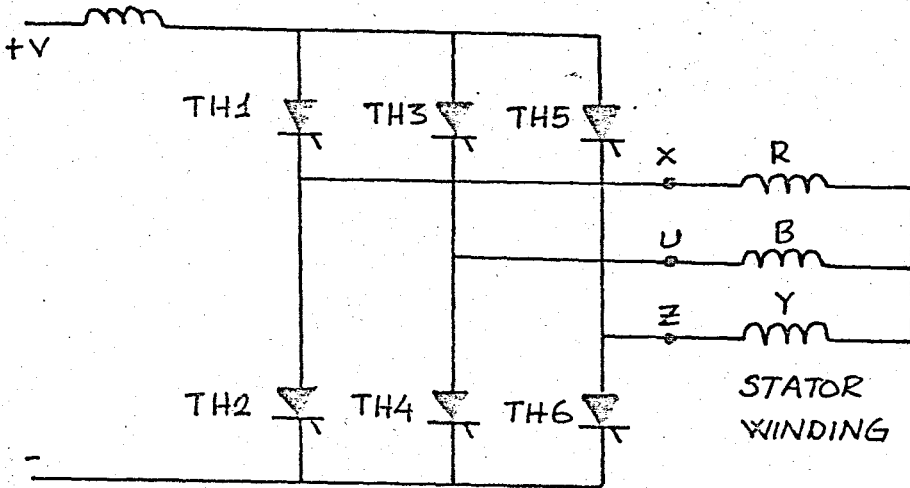


FIGURE 1.8. Three Phase Bridge Inverter.

speed around the air-gap of the motor. That speed is under the control of the thyristor circuits and they are under a programmable control, either in open or closed loop depending on what regulation is required.

The induction motor line voltages shown in Figure 1.9 are not far from sine waves. There is no even harmonics because of positive and negative half cycle symmetry. There are no third or multiples of the third harmonic because of the 60° dwell between the positive and negative waves. There are, however, fifth, seventh, eleventh, etc. harmonics which produce energy loss and torque ripples, although the mechanical dynamics will not respond to the eleventh and higher harmonic torques.

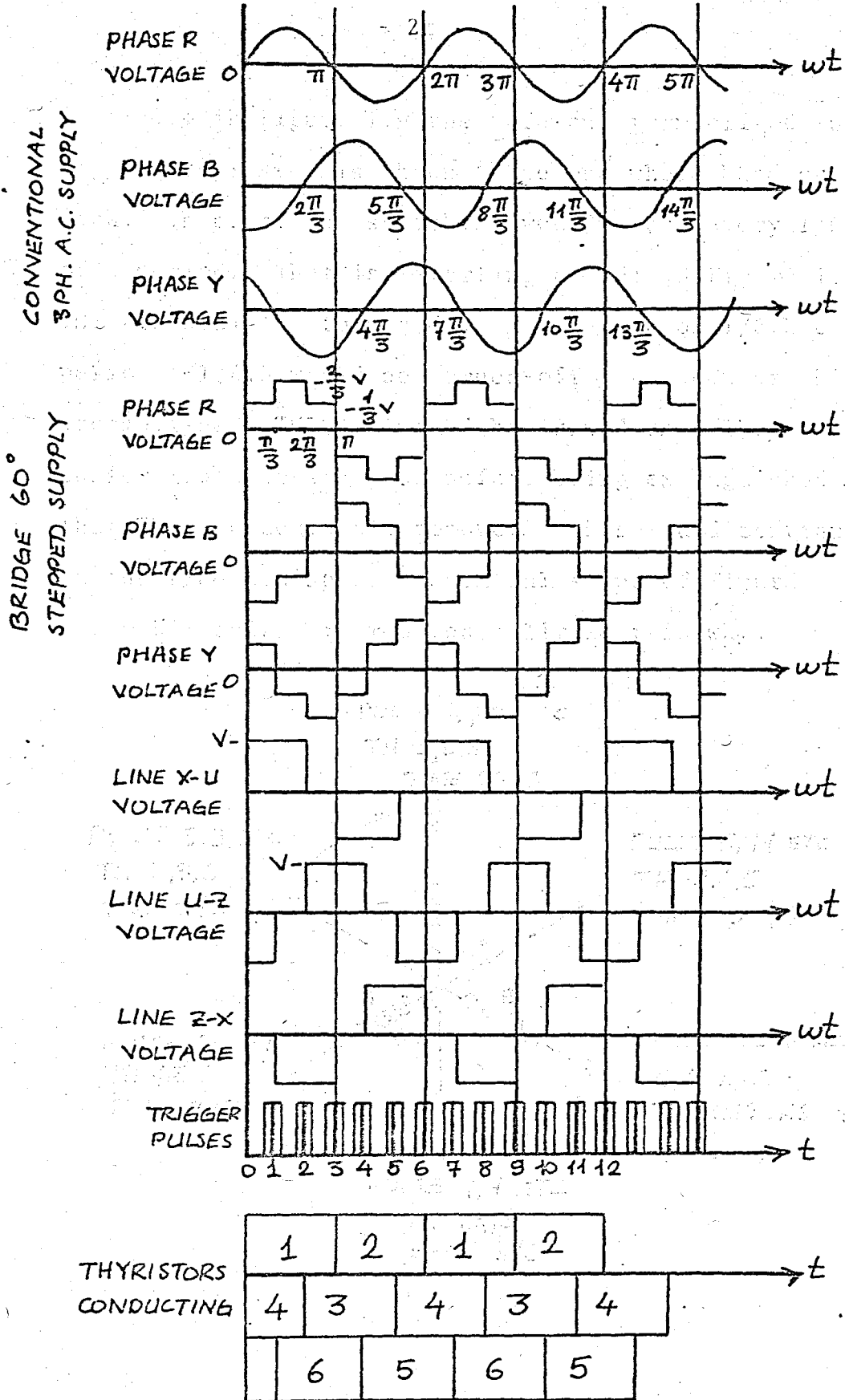


FIGURE 1.9. An Example of One Set of Inverter Waveforms and Conduction Periods.

Also in Figure 1.9 the turn-on, turn-off period of any one thyristor is shown to be one whole half cycle each. In practice, switching would occur every 1/6th of a period. That is, starting at TH1 in Figure 1.8, TH1,4,5 would be turned on. At the end of 1/6th of a period TH1,4,5 would be turned-off. As soon as this is accomplished, TH1,4,6 would be turned on. They would be on for 1/6th of a period before being extinguished so that TH1,3,6 could all conduct. This would continue as in the time and space sequential steps of Figure 1.10. Lower harmonics are reduced a little this way.

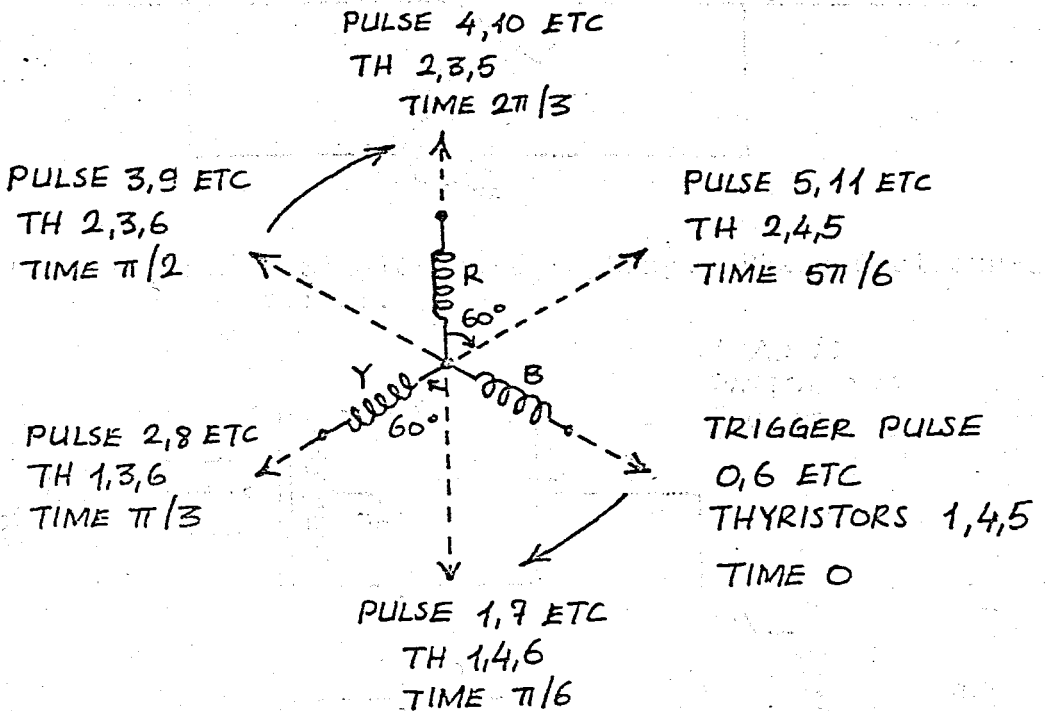


FIGURE 1.10. Stepped mmf Axes: mmf in Space with Respect to the Windings and the Thyristor Switching Sequence. The six Steps are Displaced in Space and Time by $\pi/3$ Radians (i.e., θ and ωt). The Frequency is $1/\pi$.

(c) THE CYCLOCONVERTER: The cycloconversion principle provides means of efficiently varying the frequency of the power applied to an ac motor. A cycloconverter circuit is shown in Figure 1.11a. The equivalent circuit

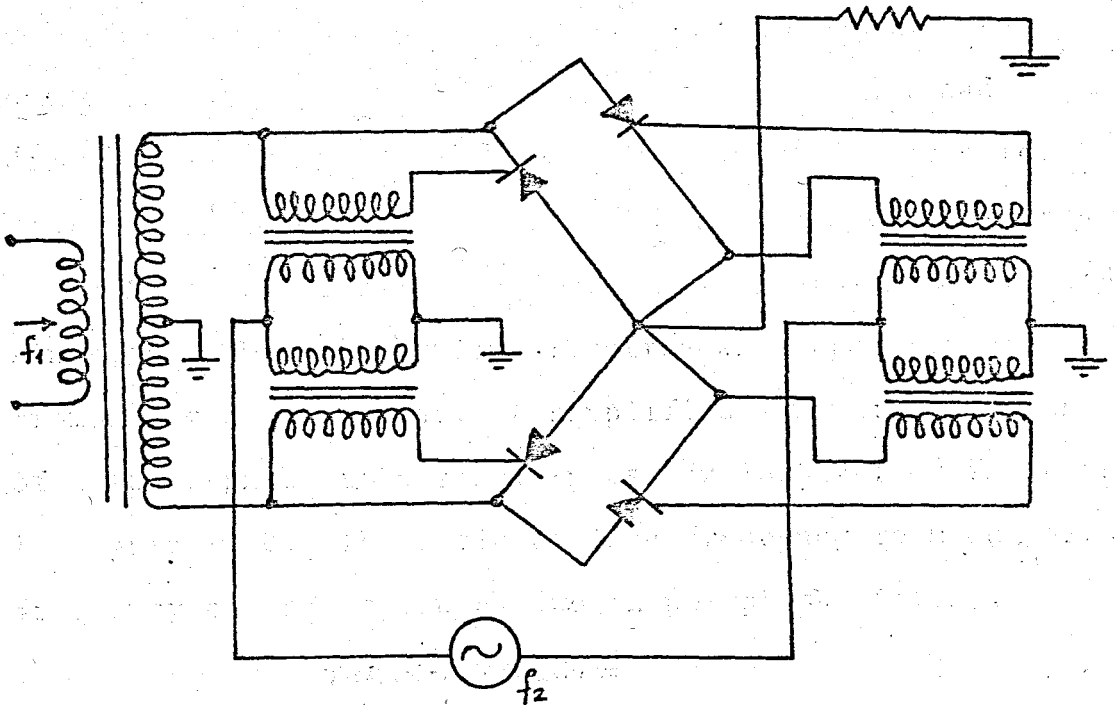
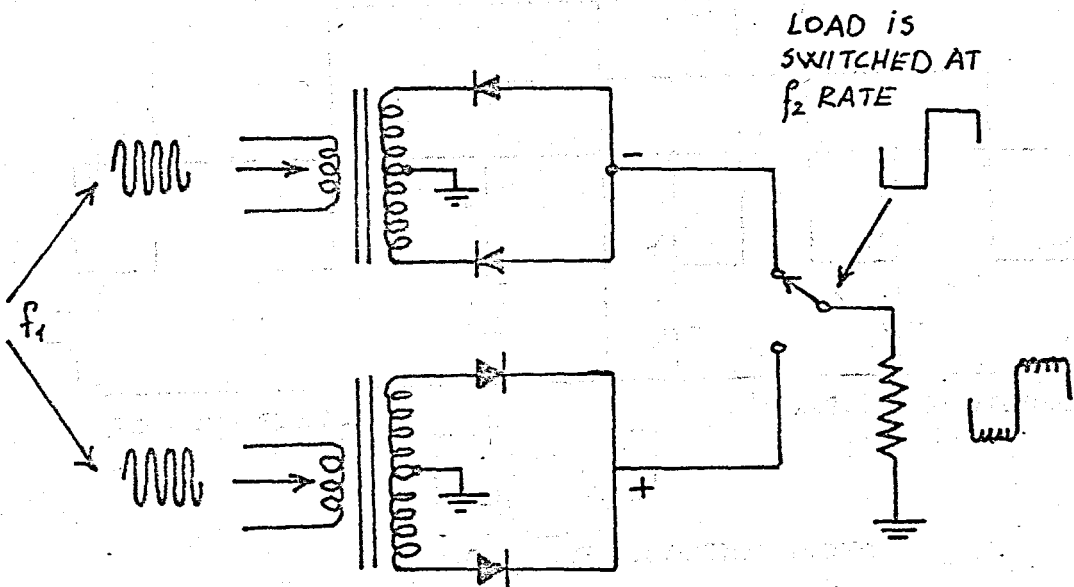


FIGURE 1.11a. A Single-Phase to Single-Phase Cycloconverter.



b. Equivalent Circuit to a.

in Figure 1.11b is useful in analyzing the operation of cycloconverters. It will be noted that two frequencies are applied to the system. One of these is f_1 , which is often obtained from the ac power line. Frequency f_1 can be considered a "carrier" modulated by the second frequency, f_2 . The output frequency is also at f_2 , and does not appear to have a waveshape desirable for motor operation. However, the inductive reactance of ac motors is sufficient to convert the current wave into a fairly good sinusoid. This is particularly true when operation is from a three-phase line. A simplified schematic diagram of a three-phase to a single-phase cycloconverter is shown in Figure 1.12. The ratio of line frequency to modulation frequency can be as low as two in polyphase systems.

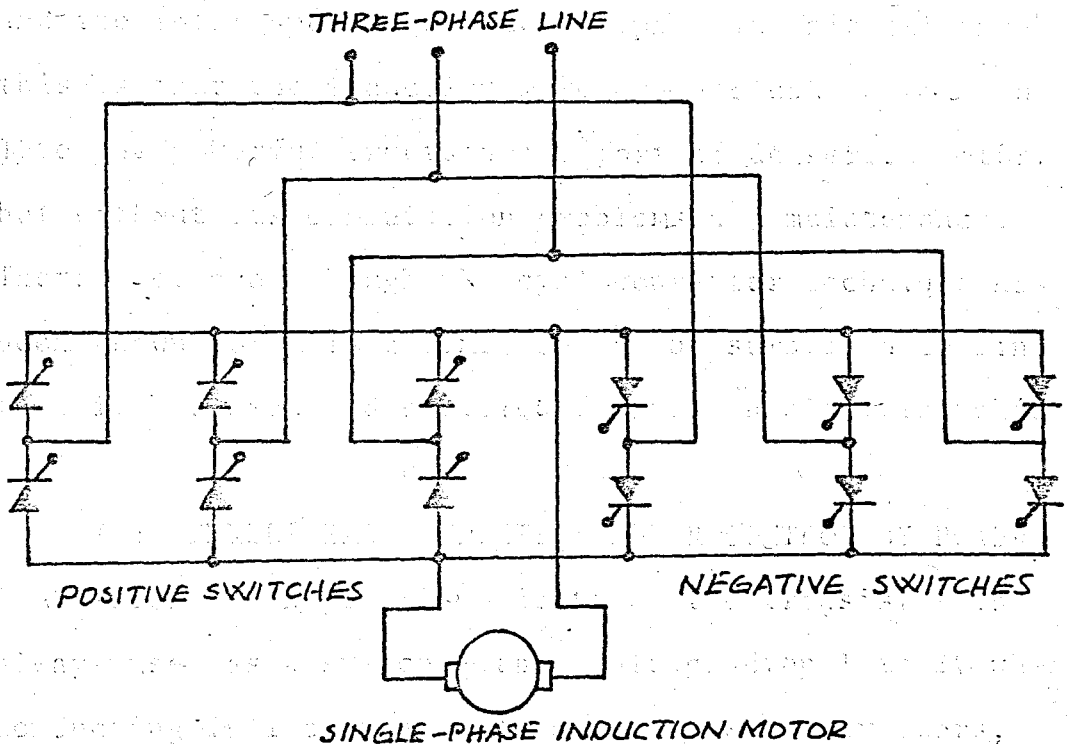


FIGURE 1.12. A 3-Phase to Single-Phase Cycloconverter.

With the cycloconverter, an induction motor can be operated from zero speed to one-third, and in some cases one-half, the speed that would otherwise be obtained from the power-line frequency. In addition to providing efficient and continuous speed control, the cycloconverter enables an induction motor to develop maximum torque at slow speeds. It is fortunate that induction motors develop maximum torque at a certain slip speed, regardless of the actual speed of the rotor. Thus, if maximum torque corresponds to a slip speed of 50 rpm when the rotor is turning at 1740 rpm, the maximum torque is available when the rotor turns at a much slower speed. This is achieved when the stator is fed with a frequency which makes the difference between the rotating magnetic field and the rotor speed equal to 50 rpm. The significance of this is that the induction motor can be caused to simulate the powerful tructional effort of dc series motor. but without its commutation problems and maintenance. Therefore, even though the cycloconverter technique has been known for a long time, do not be surprised to find that it has been rediscovered for use in electric vehicles.

(d) THREE-PHASE INDUCTION MOTOR CONTROL BY POWER TRANSISTORS: In power applications the transistor is always used as a switch with a voltage drop 1 to 2V when conducting full current. In static power convertors, the waveform is often a square or quasi-square wave. This

can be generated by transistors. The scheme used in this thesis is based on this principle and will be explained in detail in the next chapter.

CHAPTER 2

THEORY OF OPERATION OF THE TRANSDUCER

The theory of operation of the transducer is based on the principle of the photoconductive cell. The photoconductive cell is a semiconductor material which changes its electrical resistance when it is exposed to light. The resistance of the photoconductive cell is high in the dark and low when it is exposed to light. The change in resistance is due to the generation of electron-hole pairs in the semiconductor material. The photoconductive cell is used as a detector of light in the transducer. The light from the source is focused on the photoconductive cell by a lens. The change in resistance of the photoconductive cell is converted into a change in voltage by a bridge circuit. The change in voltage is then amplified by an operational amplifier. The output of the operational amplifier is a voltage which is proportional to the intensity of the light. The output voltage is then converted into a current by a current-to-voltage converter. The current is then measured by a current meter. The current meter is a device which converts a current into a deflection of a needle on a scale. The deflection of the needle is proportional to the current. The current is proportional to the intensity of the light. Therefore, the deflection of the needle is proportional to the intensity of the light. The transducer is used to measure the intensity of light in the experiment.

The transducer is used to measure the intensity of light in the experiment. The intensity of light is measured by the deflection of the needle on the scale of the current meter. The deflection of the needle is proportional to the current, which is proportional to the intensity of the light. The transducer is used to measure the intensity of light in the experiment.

CHAPTER 2

POWER TRANSISTORS IN VARIABLE SPEED DRIVES

Since the mid-1960's, thyristors have become established as the power control element in applications from domestic lighting and washing-machine controllers to d.c. rolling-mill drives and inverters for alternator starting, with ratings up to at least 10 MW. During this period, transistors were also evolving into types suitable for power control. Today, British-developed 500V 300A transistors are being applied to d.c. servo drives and inverters for multiple-unit traction drives. In application to both a.c.- and d.c.-motor drives, the fast switching capability of transistors can have advantages over thyristors, and we shall see it grow as an alternative power controller.

2.1. POWER TRANSISTORS IN SPEED CONTROL SYSTEMS

Transistors are generally considered as amplifier components for radio and other signals, oscillator or logic elements, and, increasingly, as the building blocks

for integrated circuitry and microprocessors. For power applications, the hi-fi-amplifier output stages comes to mind rather than industrial drives; however, when one considers ear-crippling sound of certain establishments, it is apparent that simultaneous heat, light and power ought to be possible!

Industrially useful transistors were produced because of the need to replace the line-output valves of television sets by transistors, which had already displaced valves from the rest of the set by about 1968. The resulting 400V 10A transistor was realized to have other applications.

In power applications the transistor is always used as a switch with a voltage drop of 1 to 2V when conducting full current as shown in Figure 2.1. If the base current of the VX26014 is less than 10A, it will come out of saturation at some lower current, e.g., 60A: any increase in load will cause excessive dissipation and probably, damage. At 110A and 1.8V the transistor will still need substial heatsink, and also, to decrease base drive, it is usually used in a Darlington connection with a current gain of at least times 100. When switched off, the transistor has a thermally dependent leakage current that increases exponentially with temperature, and may be a few milliamperes at 25°C in a 50A in device.

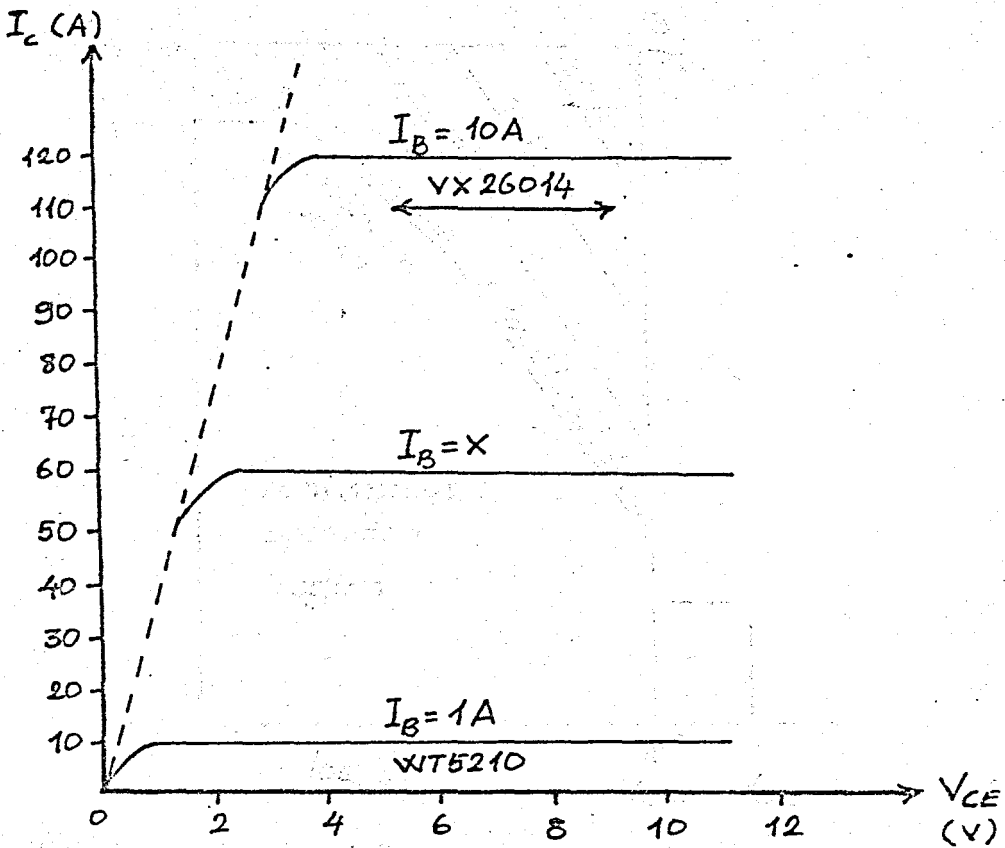


FIGURE 2.1. I_C and V_C Characteristics of Power Transistors.

In operation, the transistor switches between "on" and "off" states, and for this type of operation a safe-operating-area diagram is provided. In Figure 2.2 region A defines the range of collector current and voltage for continuous working with its boundaries as indicated. When the transistion time is decreased, the switching locus can move into B and pass into the extremely high dissipation corner if the switching is complete in a few microseconds. The maximum peak collector current is usually only some 25% greater than the continuous maximum current I_{Cmax} giving much less margin than thyristors.

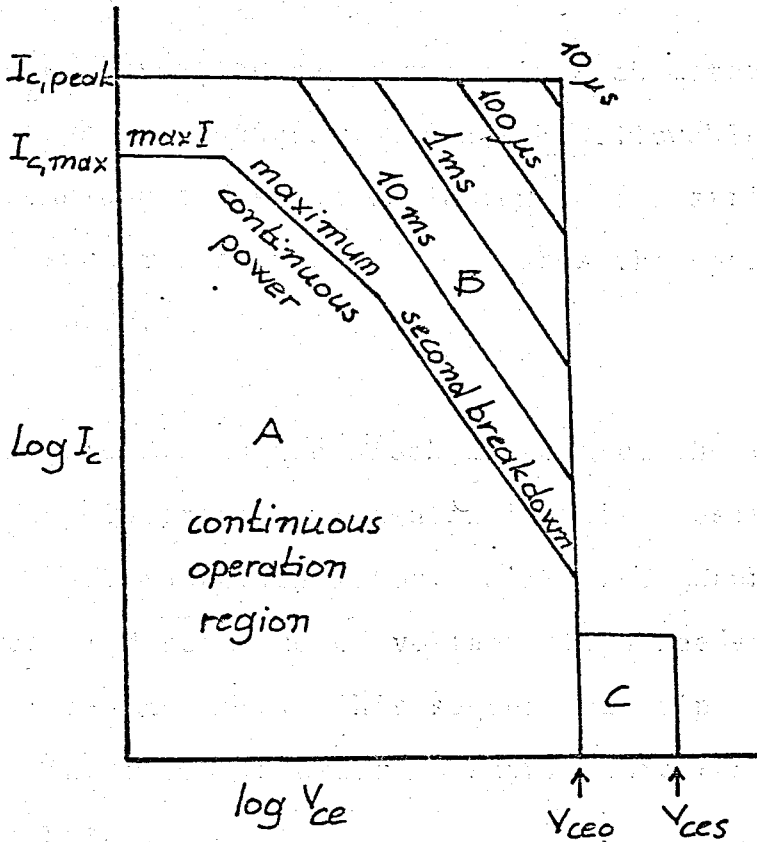


FIGURE 2.2. Typical Safe Operation Area (s.o.a.r.) Diagram.

Industrially, the squirrel-cage induction motor is the most widely used drive, running with a regulation of from 5 to 10% from no load to full load. Since its speed derives from a rotating field of angular frequency determined by the supply, it follows that a variable frequency supply is needed for a wide range of motor speed. If the frequency is reduced below the nominal 50 Hz, the magnetic circuit will maintain full flux for less supply voltage and conversely an increase in frequency above 50 Hz will require extra voltage to sustain full flux and full torque rating. Consequently, for operation over a wide speed range, both motor voltage and frequency are controlled. In small motors, this basic requirement can be circum-

vented by inserting resistances in each motor lead. However, such a technique would not be allowable with large motors unless the speed variation were restricted. The use of such resistance also degrades the speed regulation of the motor.

Figure 2.3 is the block diagram of the variable-frequency inverter implemented in this thesis up to 5H three-phase induction motor. Six power channels provide the required sequence of voltage steps needed to develop the quasi-sine wave. This sequence is repeated at 120-degree intervals in order to supply three-phase energy to the motor.

The three-phase wave synthesis imparted by the digital logic modules commences with the CL_1 pulse train. The subsequent modifications made to these pulses, together with various combining techniques, are illustrated in the logic-timing sequence shown in Figure 2.4. It is well to note that a basic three-phase wave already exists with respect to waves A, B and C. 50 logic operates as a 3-bit shift register. It should be noted that the shift register provides complement waves A', B' and C' as well. The complement waves are used in the building-block to modify the original ABC three-phase waves. One desired modification is a reduction in the half-wave duty cycle to 165 degrees from the normal 180 degrees. This prevents simultaneous conduction of power output

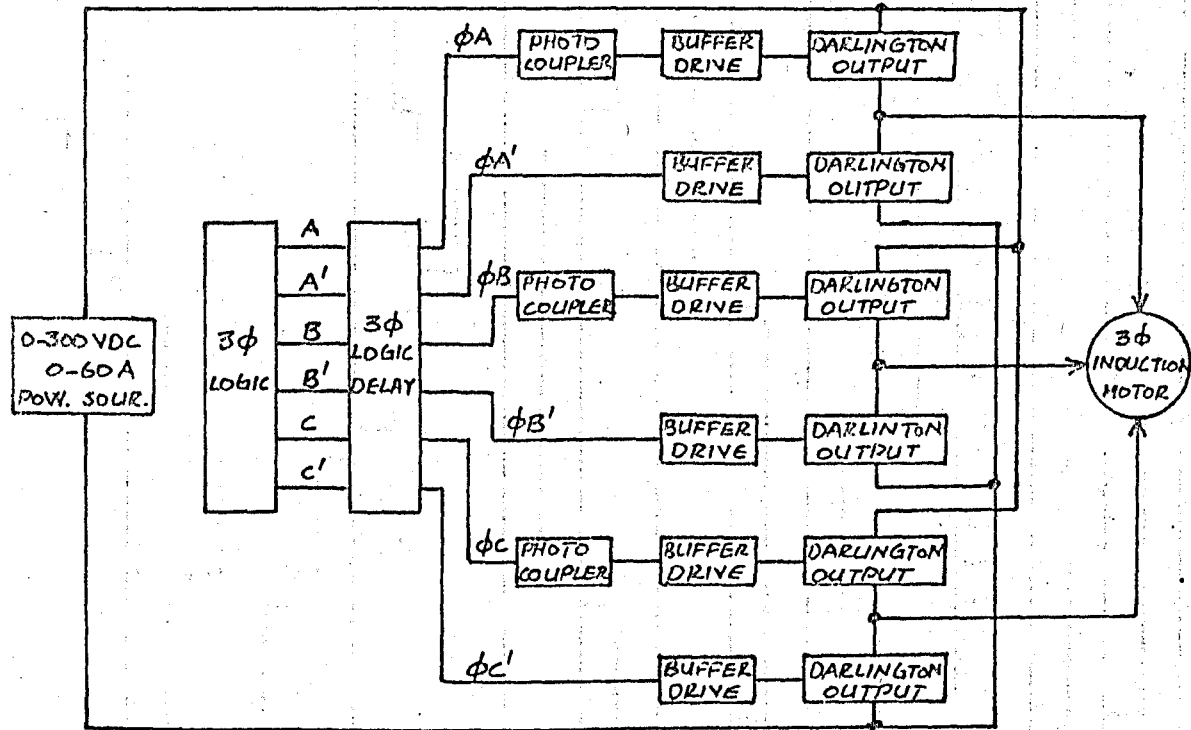


FIGURE 2.3. Block Diagram of a Variable-Frequency Inverter for Speed Control of a 3-Phase motors.

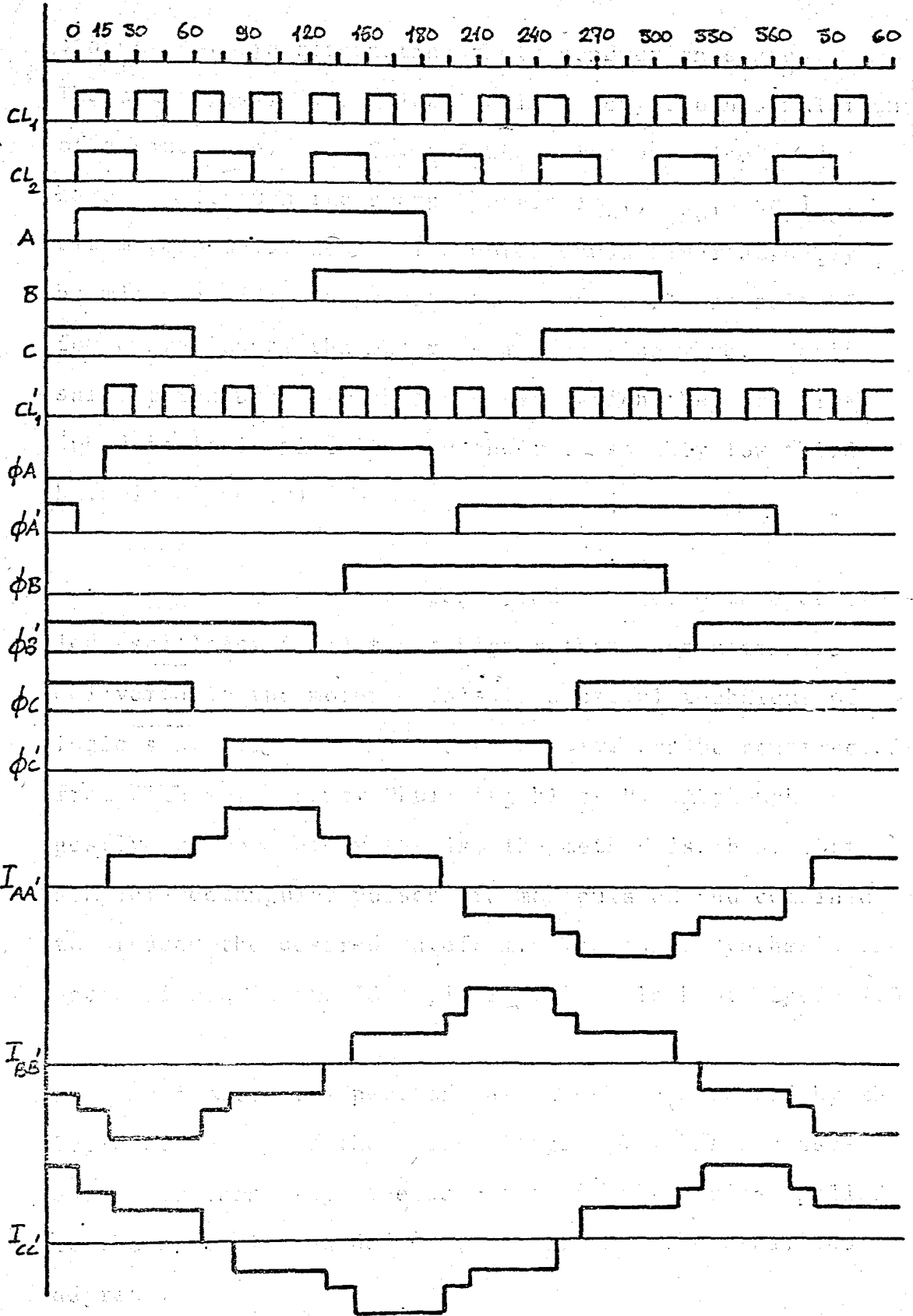


FIGURE 2.4. Logic Timing Sequence for Variable-Frequency Inverter.

stages that are alternating their conduction states. The other desired modification is a very rough simulation of a sine wave. The CL_1 and CL_2 waves are also used here. (Although the stepped waves $I_{AA'}$, $I_{BB'}$ and $I_{CC'}$ ultimately delivered to the motor could never actually be mistaken for sine waves, they are nearly as suitable for operation of the motor as a true sine wave. Their salient features are the ease with which they are produced in logic circuits and their reasonably low third-harmonic content:)

The basic frequency generated by the voltage controlled oscillator is 24 times higher than that ultimately delivered to the motor. This is a useful technique of logic synthesis. A low-frequency wave can be constructed from higher-frequency "building blocks". Although suggestive of Fourier synthesis, the method is this, that simpler-rectangular pulses are manipulated and combined to produce the desired waveform. The pulse synthesis is accomplished in the 30 logic function block of Figure 2.3.

An important aspect of the waveshape produced by the logic circuitry is the zero-voltage step. As a consequence of this step, the duration of half cycles applied to the motor is 165 degrees, rather than the usual 180 degrees.

The function block that produces this zero-voltage

step is the 3 ϕ logic delay in Figure 2.3. Photocouplers provide electrical isolation between the three-phase logic circuitry and the motor-drive circuits.

The Darlington output blocks generate 3 ϕ currents, that are delivered to the motor. There is much repetition in the circuit configuration. Not only are all circuits for each of the three phases identical, but each of the six power channels contain five Darlington output amplifiers connected in parallel.

The external dc power supply should have a current capability of about 60 amperes and should permit variation of its output voltage from 0 to 300 volts. Such requirements are best served by a voltage-regulated switching supply which minimizes power dissipation. An alternative is a simple full-wave power supply with autotransformer control in the power line. A single phase power line can be used for dc supply, but three-phase, 60 or 50 Hz power would probably be more practical. When the dc supply is adjusted for 220 volts, the motor receives three-phase power at 50 Hz. With 20 volts from dc supply, the three-phase power supplied to the motor has a frequency of 5 Hz. The speed range corresponding to such a voltage reduction is approximately 1420 rpm to 142 rpm for four poles motor. The design, the implementation and the characteristics of each block are explained in detail in the following section.

2.2. A UNIJUNCTION TRANSISTOR PULSE GENERATOR CIRCUIT AND WAVE SHAPER

The block diagram of Voltage Controlled Oscillator and Wave Shaper is shown in Figure 2.5a. A simple pulse generator using a unijunction transistor is shown in Figure 2.5b. The typical waveforms are shown in Figure 2.5c. Assuming that the capacitor is initially uncharged, the voltage at point X begins to rise in an exponential manner until it reaches the peak-point voltage of the U.J.T. At this instant of time, the U.J.T. switches to its low resistance conducting mode and the capacitor is discharged through the resistor R_1 causing a positive going pulse to be generated at Y. The pulse repetition rate is controlled by the value of R, since this controls the time constant RC of the capacitor charging circuit, and the pulse width by R_1 since this affects the discharge time constant.

Assuming that the capacitor is initially uncharged, then the voltage at point X prior to breakdown is given by

$$V_X = V_{BB} (1 - e^{-t/RC})$$

where RC is the charging time constant of the resistor capacitor circuit, and t is the time from the commencement of the waveform. Discharge occurs when V_X is equal to

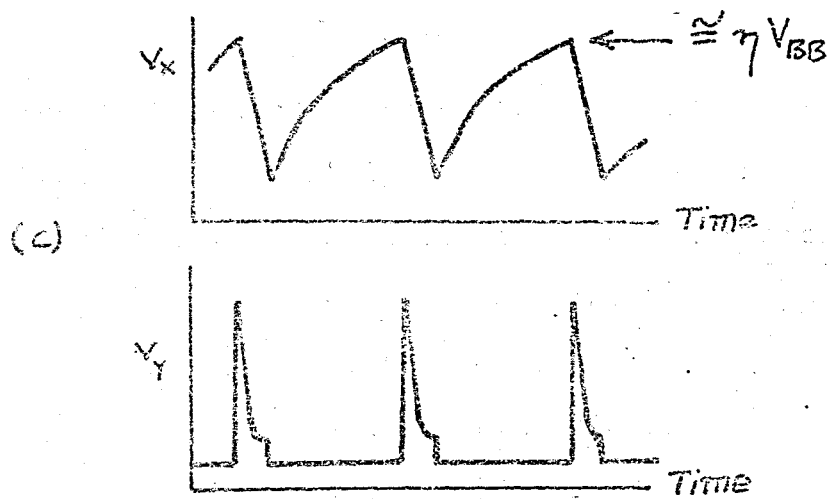
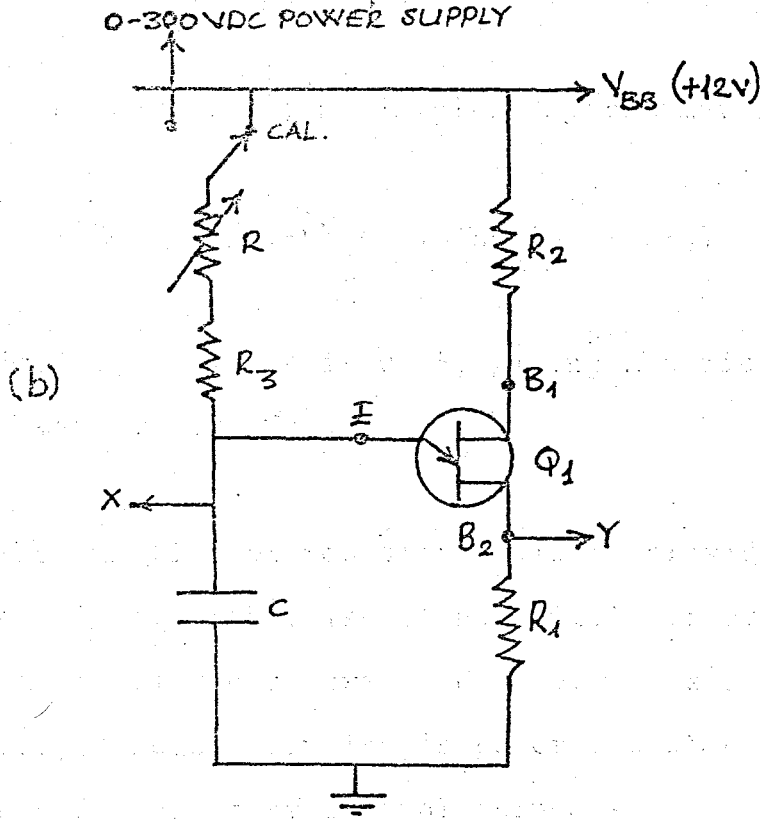
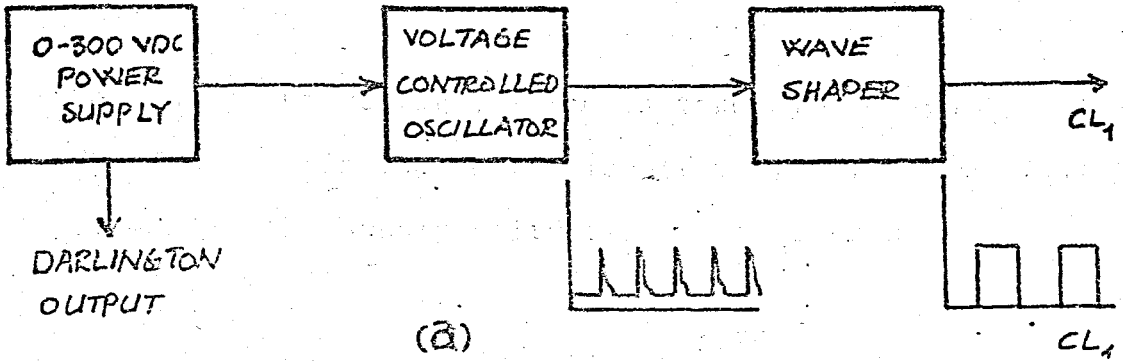


FIGURE 2.5. (a) The Block Diagram of V.C.O and Wave Shaper; (b) A Simple Pulse Generator Using a U.J.T.; (c) The Typical Waveforms.

the peak-point voltage, which is taken to be equal to nV_{BB} (where n is the intrinsic-off ratio of the U.J.T., and V_{BB} is the supply voltage). That is when

$$nV_{BB} = V_{BB}(1 - e^{-t/RC})$$

Hence, the periodic time is given approximately by

$$t = RC \ln 1/(1-n) = 2.3 RC \lg 1/(1-n)$$

A typical value for n is 0.55, giving a periodic time of approximately 0.8 RCs.

The function of resistor R_2 is to provide temperature stability, otherwise it has little effect upon the performance of the circuit. However, as a result of this resistor, a negative pulse is generated at base-two and can be used for other control purposes.

The pulse which is generated at point Y is of short duration, being typically 10 μ s to 15 μ s, and may be coupled directly to the wave shaper of the circuit. Hence, we obtain these values for our circuit (see Appendix 1)

$$R = 100 \text{ k}\Omega \quad R_5 = 220 \text{ k}\Omega$$

$$R_1 = 560\Omega \quad R_2 = 220\Omega$$

$$C = 0.05 \text{ }\mu\text{F}$$

The circuit was calibrated such that at 220V dc input, the output frequency is 1200 Hz corresponding to a final 3 ϕ output voltage of 50 Hz. As the supply voltage is decreased the output frequency decreases linearly down to 168 Hz at 30 Volts. In this wave the requirement that V/f stays constant is achieved. (See Section 3.2)

Wave Shaper: Figure 2.6 shows the Wave Shaper. The transistor amplifies the pulses which are generated by U.J.T, and then these pulses are applied to a J-K type Flip-Flop. The inputs of Flip-Flop are such that J:1, K:1, R:0, S:0. In this way at Q output of the J-K flip-flop the clock signal for the rest of the circuitry is obtained. The frequency of the clock is half of that of the U.J.T. output.

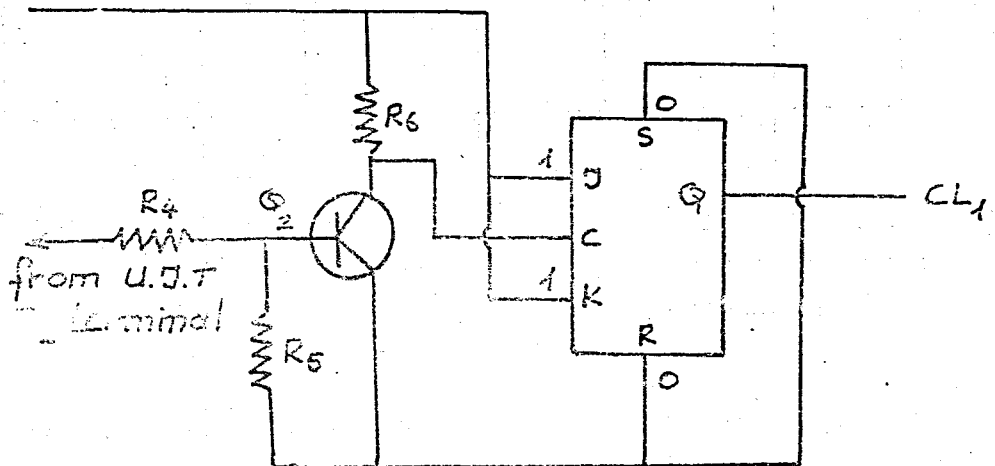


FIGURE 2.6. Wave Shaper.

ter. It is assumed that all flip-flops are initially in their 0 states. We apply J:1, C: first clock of CL_1 , K:1, S:0, R:0 of FF1. Then Q of FF1 goes to the 1 state. (See Appendix 2, Truth Table of J-K Flip Flop.) When the second positive going clock CL_1 signal is applied to the FF1, then FF1 will change the state and Q of FF1 goes to 0 state. This process continues, and we get CL_2 wave form on the output of FF1.

When the first positive-going clock signal of CL_2 is applied to FF2, the inputs of FF2 are such that: J:0, C:CP1 of CL_2 , K:0, S:0, R:0, then Q of FF2 goes to 1 state. Let us denote this waveform by A. The second positive-going clock signal of CL_2 will be applied to J of FF3, and A will not change. Hence, the inputs of FF3 are, J:1, C:CP2 of CL_2 , K:0, S:0, R:0, and Q of FF3 goes to 1 state, and \bar{Q} of FF3 goes to 0 state. Let \bar{Q} of FF3 be C, and there is not change in the waveform of A again.

The third positive-going clock signal of CL_2 is applied to FF4, then the inputs of FF4 are as follows: J:1, C:CP3 of CL_2 , K:0, R:0, S:0, and Q of FF4 goes to 1 state. The waveform at the Q output of FF4 is denoted by the symbol B, and this process continues so that we get the waveforms, A,B,C as shown in Figure 2.8b. We see that the waveforms A,B,C are shifted 120 degrees.

	FF2	FF3	FF4	FF2	FF3	FF4	FF2	FF3	FF4
J	1	1	1	0	0	0	1	1	1
C	CP1	CP2	CP3	CP4	CP5	CP6	CP7	CP8	CP9
K	0	0	0	1	1	1	0	0	0
R	0	0	0	0	0	0	0	0	0
S	0	0	0	0	0	0	0	0	0
†	0	0	0	1	1	1	0	0	0
Q	1(A)	1(C')	1(B)	0	0	0	1	1	1
*Q̄	0(A')	0(C)	0(B')	1	1	0	0	0	0'

FIGURE 2.8a. Truth Table 3-Bit Shift Register.
 († : Present State, *: Next State)

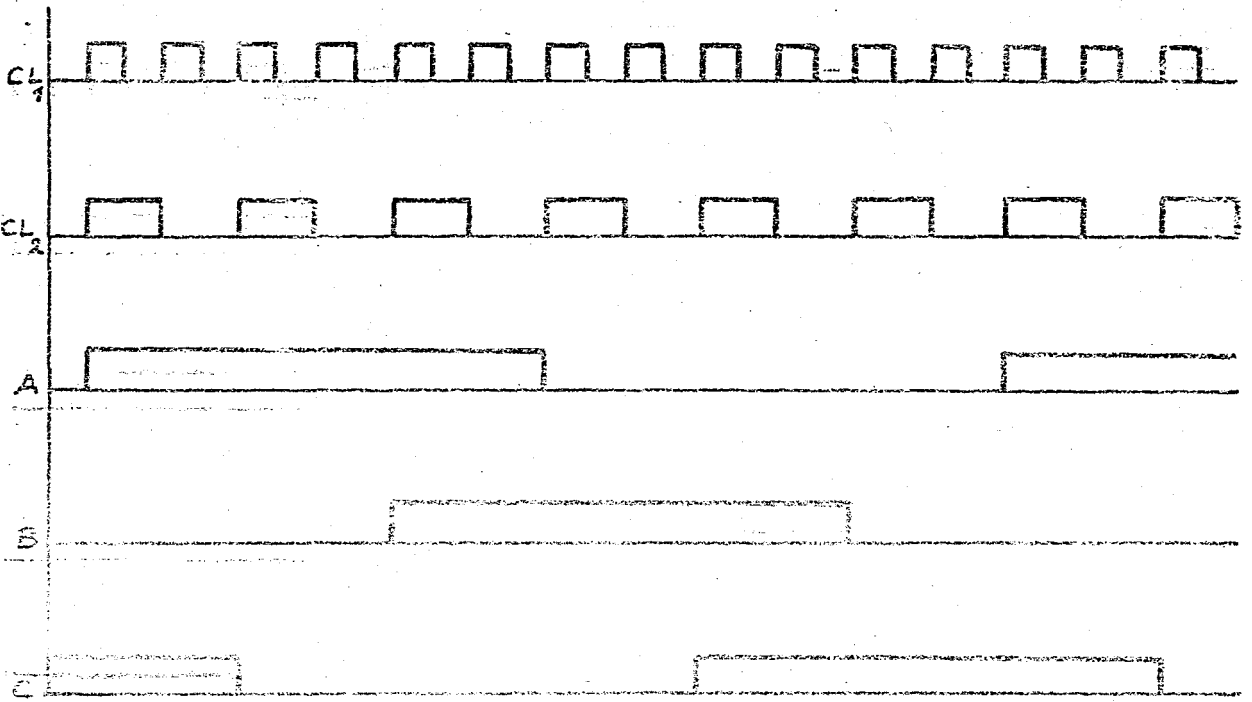


FIGURE 2.8b. The Waveforms of Three-Bit Shift Register.

It should be noted that the shift register also provides complement waveforms A', B', C'. These complement waves are used in the building-block process to modify the original ABC three-phase waves. The NAND gates inhibit forbidden-state operation of the shift register.

2.4. 3 \emptyset LOGIC DELAY

3 \emptyset Logic Delay is used to modify the original ABC three-phase waves. This modification is a reduction in the half-wave duty-cycle to 165 degrees from the normal 180 degrees. An important aspect of the waveshape produced by the logic circuitry is the zero-voltage step. As a consequence of this step, the duration of half cycles applied to the motor is 165 degrees, rather than the usual 180 degrees. This prevents conduction overlap between power-output stages that are turning off and those that are turning on. The function block that produces this zero-voltage step is 3 \emptyset Logic Delay in Figure 2.3. The waveforms of 3 \emptyset Logic are shown in Figure 2.9 and the truth table of 3 \emptyset logic delay is shown in Figure 2.10. Photocouplers provide electrical isolation between the three-phase logic circuitry and the motor-drive circuits. D type Flip-Flops are used in 3 \emptyset logic circuit and the clock pulses are CL₁'.

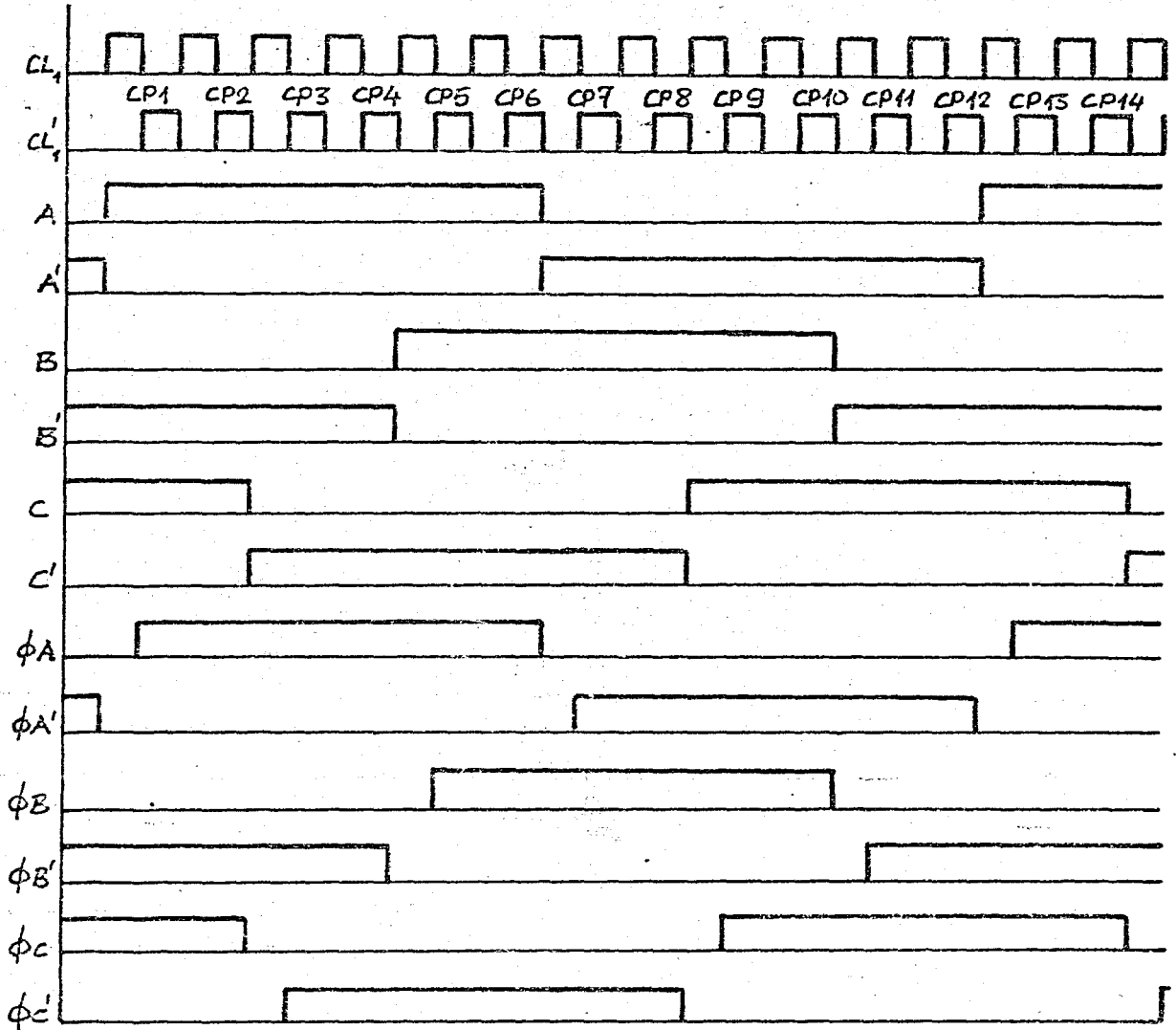


FIGURE 2.9. The Waveforms of 3Ø Logic Delay.

2.5. DARLINGTON OUTPUT

The Dalington output contains six power channels. The signal of 3Ø logic delay ϕA , $\phi A'$, ϕB , $\phi B'$, ϕC , $\phi C'$ trigger the Darlington Transistors. The circuit configuration for various motors with different power ratings is basically the same. The number of Darlington transistors

INPUTS		CP1	CP2	CP2 ^x	CP3	CP4	CP4 ^x	CP5	CP6	CP6 ^x	CP7	CP8	CP8 ^x	CP9	CP10	CP10 ^x	CP11	CP12	CP12 ^x	CP13	CP14	CP14 ^x	CP15	CP16	CP16 ^x	CP17
FF 5 (ϕA)	D	1	1	1	1	1	1	1	1	0	0	0	0	0	0	0	0	0	1	1	1	1	1	1	1	1
	R	0	0	0	0	0	0	0	0	1	1	1	1	1	1	1	1	1	0	0	0	0	0	0	0	0
	S	0	0	0	0	0	0	0	0	0	0	0	0	0	0	0	0	0	0	0	0	0	0	0	0	0
	Q	1	1	1	1	1	1	1	1	0	0	0	0	0	0	0	0	0	0	1	1	1	1	1	1	1
	\bar{Q}	0	0	0	0	0	0	0	0	1	1	1	1	1	1	1	1	1	1	0	0	0	0	0	0	0
FF 6 ($\phi A'$)	D	0	0	0	0	0	1	1	1	1	1	1	1	1	1	0	0	0	0	0	0	0	0	0	0	1
	R	1	1	1	1	1	0	0	0	0	0	0	0	0	0	1	1	1	1	1	1	1	1	1	1	0
	S	0	0	0	0	0	0	0	0	0	0	0	0	0	0	0	0	0	0	0	0	0	0	0	0	0
	Q	0	0	0	0	0	0	1	1	1	1	1	1	1	1	0	0	0	0	0	0	0	0	0	0	1
	\bar{Q}	1	1	1	1	1	1	0	0	0	0	0	0	0	0	1	1	1	1	1	1	1	1	1	1	0
FF 7 (ϕB)	D	0	0	0	0	0	1	1	1	1	1	1	1	1	1	0	0	0	0	0	0	0	0	0	0	1
	R	1	1	1	1	1	0	0	0	0	0	0	0	0	0	1	1	1	1	1	1	1	1	1	1	0
	S	0	0	0	0	0	0	0	0	0	0	0	0	0	0	0	0	0	0	0	0	0	0	0	0	0
	Q	0	0	0	0	0	0	1	1	1	1	1	1	1	1	0	0	0	0	0	0	0	0	0	0	1
	\bar{Q}	1	1	1	1	1	1	0	0	0	0	0	0	0	0	1	1	1	1	1	1	1	1	1	1	0
FF 8 ($\phi B'$)	D	1	1	1	1	1	0	0	0	0	0	0	0	0	0	1	1	1	1	1	1	1	1	1	1	0
	R	0	0	0	0	0	1	1	1	1	1	1	1	1	1	0	0	0	0	0	0	0	0	0	0	1
	S	0	0	0	0	0	0	0	0	0	0	0	0	0	0	0	0	0	0	0	0	0	0	0	0	0
	Q	1	1	1	1	1	0	0	0	0	0	0	0	0	0	0	1	1	1	1	1	1	1	1	1	0
	\bar{Q}	0	0	0	0	0	1	1	1	1	1	1	1	1	1	0	0	0	0	0	0	0	0	0	0	1
FF 9 (ϕC)	D	1	1	0	0	0	0	0	0	0	1	1	1	1	1	1	1	1	1	1	1	0	0	0	0	0
	R	0	0	1	1	1	1	1	1	1	0	0	0	0	0	0	0	0	0	0	0	0	1	1	1	1
	S	0	0	0	0	0	0	0	0	0	0	0	0	0	0	0	0	0	0	0	0	0	0	0	0	0
	Q	1	1	0	0	0	0	0	0	0	0	1	1	1	1	1	1	1	1	1	1	0	0	0	0	0
	\bar{Q}	0	0	1	1	1	1	1	1	1	1	0	0	0	0	0	0	0	0	0	0	0	1	1	1	1
FF 10 ($\phi C'$)	D	0	0	1	1	1	1	1	1	1	0	0	0	0	0	0	0	0	0	0	0	1	1	0	0	0
	R	1	1	0	0	0	0	0	0	0	0	1	1	1	1	1	1	1	1	1	1	0	0	0	0	0
	S	0	0	0	0	0	0	0	0	0	0	0	0	0	0	0	0	0	0	0	0	0	0	0	0	0
	Q	0	0	0	1	1	1	1	1	1	1	0	0	0	0	0	0	0	0	0	0	0	1	1	1	1
	\bar{Q}	1	1	1	0	0	0	0	0	0	0	1	1	1	1	1	1	1	1	1	1	1	0	0	0	0

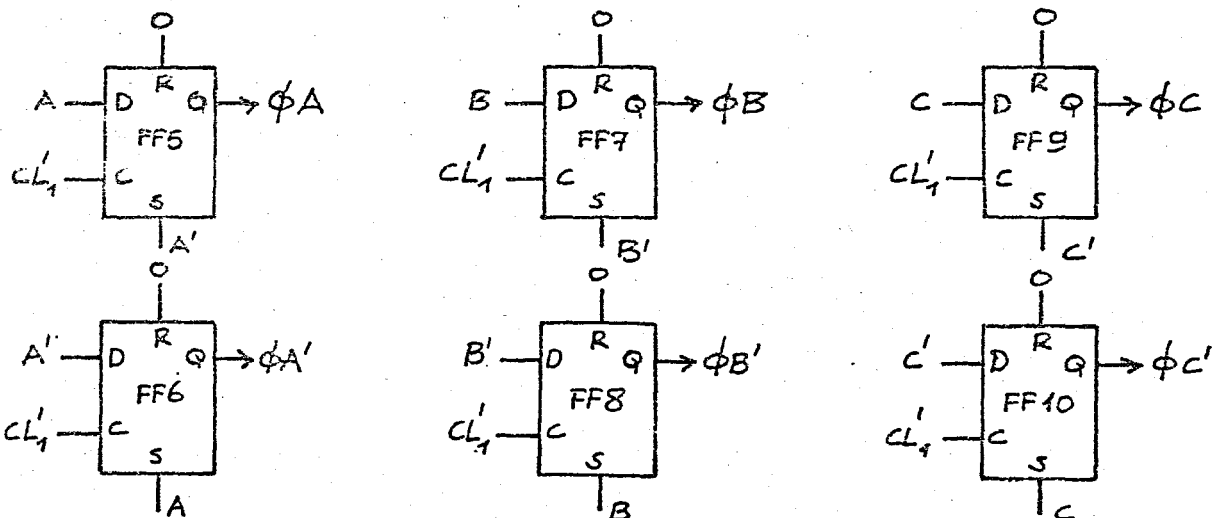


FIGURE 2.10. Truth Table of 30 Logic Delay.

required is determined by the rating of the motor whose speed is to be controlled. The circuit configuration for each one of the three phases is also identical. In the implementation for this thesis 3 Darlington transistors (BD699) were used in each one of 6 channels having a rating of 80 volts, 5Amps. However, the construction is such that these can easily be replaced by 400 Volts transistors to enable outputs of greater than 50 Hz.

Buffer drives amplify the current of ϕA , $\phi A'$, ϕB , $\phi B'$, ϕC , $\phi C'$ to trigger the Darlington Transistors.

The Darlington transistors can be considered as switches ϕA , $\phi A'$, ϕB , $\phi B'$, ϕC , $\phi C'$ as shown in Figure 2.12. In Figure 2.11 the operation of the Darlington transistors is explained and in Figure 2.12 a resistive load is assumed to simplify the analysis. When the load is an inductive one, the phase voltages take the form shown in Figure 2.13.

The block diagram of the Darlington outputs and the way they are connected to the motor is shown in Figure 2.14.

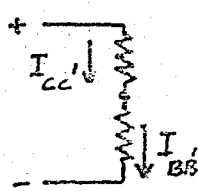
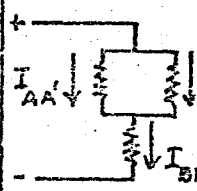
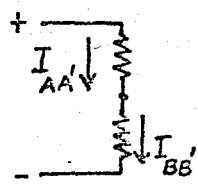
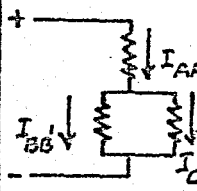
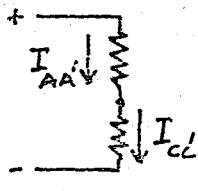
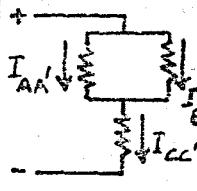
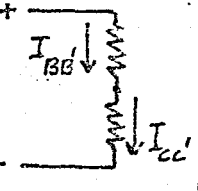
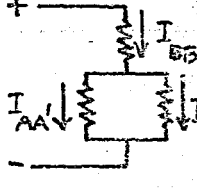
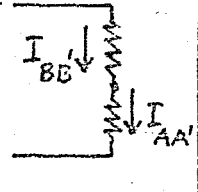
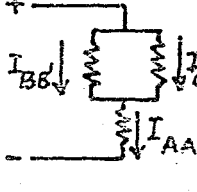
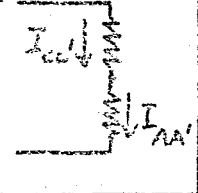
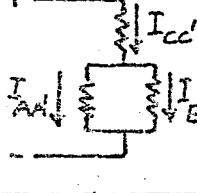
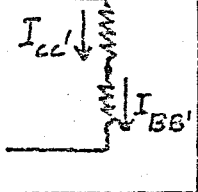
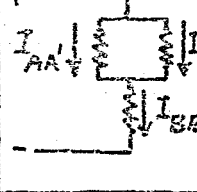
		Schematic Diagram	The current value, and way			Schematic Diagram	The current value, and way	
CASE 1	ϕA	OFF		$I_{AA'} = 0$ $I_{BB'} = I_{CC'} ; (-)$ $I_{CC'} = I_{BB'} ; (+)$	CASE 2	ON		$I_{AA'} = I_{CC'} ; (+)$ $I_{BB'} = I_{AA'} + I_{CC'} ; (-)$ $I_{CC'} = I_{AA'} ; (+)$
	$\phi A'$	OFF						
	ϕB	OFF						
	$\phi B'$	ON						
	ϕC	ON						
	$\phi C'$	OFF						
CASE 3	ϕA	ON		$I_{AA'} = I_{BB'} ; (+)$ $I_{BB'} = I_{AA'} ; (-)$ $I_{CC'} = 0$	CASE 4	ON		$I = I_{AA'} + I_{BB'} + I_{CC'} ; (+)$ $I_{BB'} = I_{CC'} ; (-)$ $I_{CC'} = I_{BB'} ; (-)$
	$\phi A'$	OFF						
	ϕB	OFF						
	$\phi B'$	ON						
	ϕC	OFF						
	$\phi C'$	OFF						
CASE 5	ϕA	ON		$I_{AA'} = I_{CC'} ; (+)$ $I_{BB'} = 0$ $I_{CC'} = I_{AA'} ; (-)$	CASES 5	ON		$I_{AA'} = I_{BB'} ; (+)$ $I_{BB'} = I_{AA'} ; (+)$ $I_{CC'} = I_{AA'} + I_{BB'} ; (-)$
	$\phi A'$	OFF						
	ϕB	OFF						
	$\phi B'$	OFF						
	ϕC	OFF						
	$\phi C'$	ON						
CASE 7	ϕA	OFF		$I_{AA'} = 0$ $I_{BB'} = I_{CC'} ; (+)$ $I_{CC'} = I_{BB'} ; (-)$	CASE 8	OFF		$I = I_{CC'} ; (-)$ $I_{BB'} = I_{AA'} + I_{CC'} ; (+)$ $I_{CC'} = I_{AA'} ; (-)$
	$\phi A'$	OFF						
	ϕB	ON						
	$\phi B'$	OFF						
	ϕC	OFF						
	$\phi C'$	ON						
CASE 9	ϕA	OFF		$I_{AA'} = I_{BB'} ; (-)$ $I_{BB'} = I_{AA'} ; (+)$ $I_{CC'} = 0$	CASE 10	OFF		$I_{AA'} = I_{BB'} + I_{CC'} ; (-)$ $I_{BB'} = I_{CC'} ; (+)$ $I_{CC'} = I_{BB'} ; (+)$
	$\phi A'$	ON						
	ϕB	ON						
	$\phi B'$	OFF						
	ϕC	OFF						
	$\phi C'$	OFF						
CASE 11	ϕA	OFF		$I_{AA'} = I_{CC'} ; (-)$ $I_{BB'} = 0$ $I_{CC'} = I_{AA'} ; (+)$	CASE 11	OFF		$I_{AA'} = I_{BB'} ; (-)$ $I_{BB'} = I_{AA'} ; (-)$ $I_{CC'} = I_{AA'} + I_{BB'} ; (+)$
	$\phi A'$	ON						
	ϕB	OFF						
	$\phi B'$	OFF						
	ϕC	ON						
	$\phi C'$	OFF						
CASE 13	ϕA	OFF		$I_{AA'} = 0$ $I_{BB'} = I_{CC'} ; (-)$ $I_{CC'} = I_{BB'} ; (+)$	CASE 13	ON		$I_{AA'} = I_{CC'} ; (+)$ $I_{BB'} = I_{AA'} + I_{CC'} ; (-)$ $I_{CC'} = I_{AA'} ; (+)$
	$\phi A'$	OFF						
	ϕB	OFF						
	$\phi B'$	ON						
	ϕC	ON						
	$\phi C'$	OFF						

FIGURE 2.11. The Operation of Darlington Outputs.

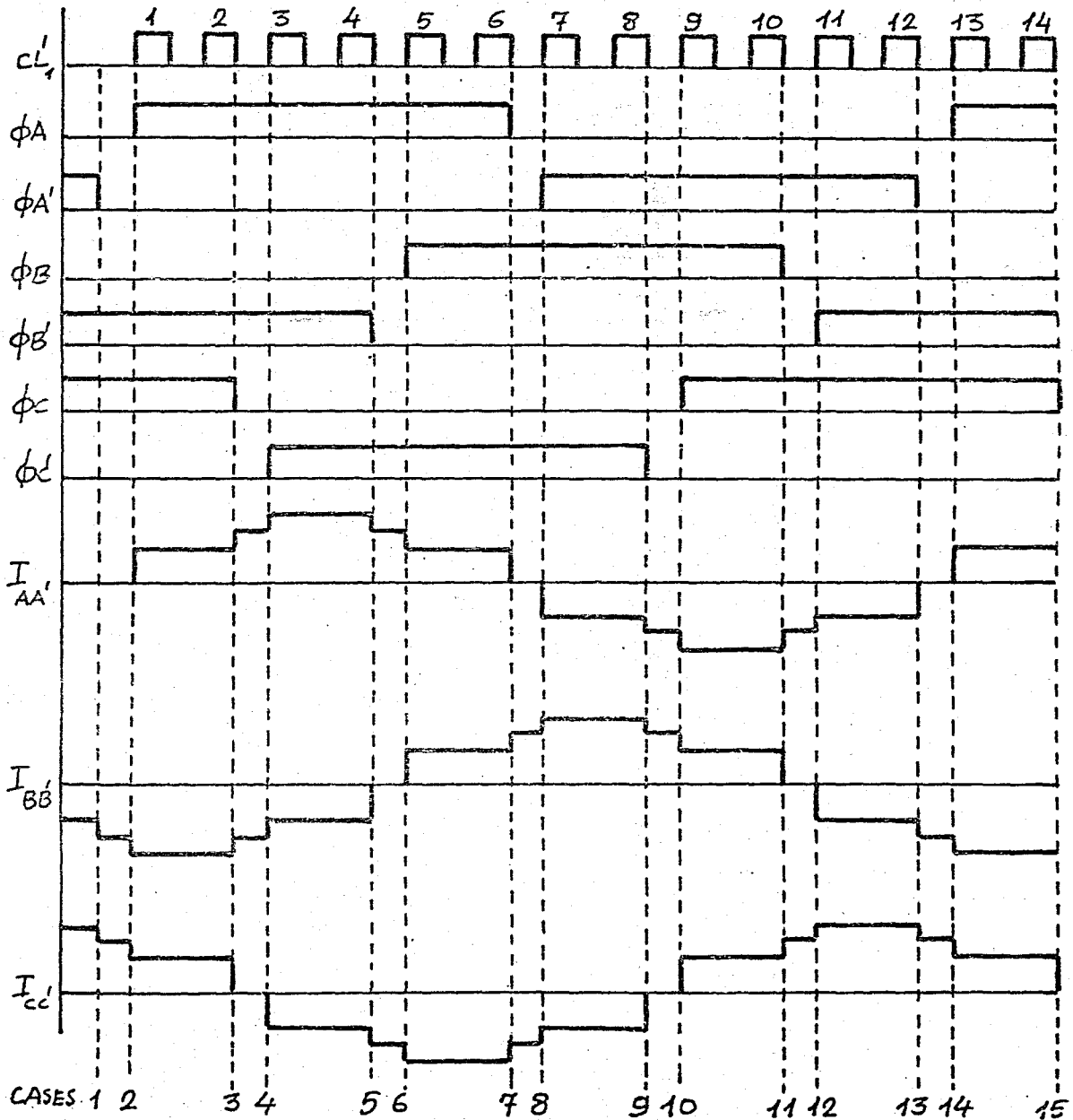
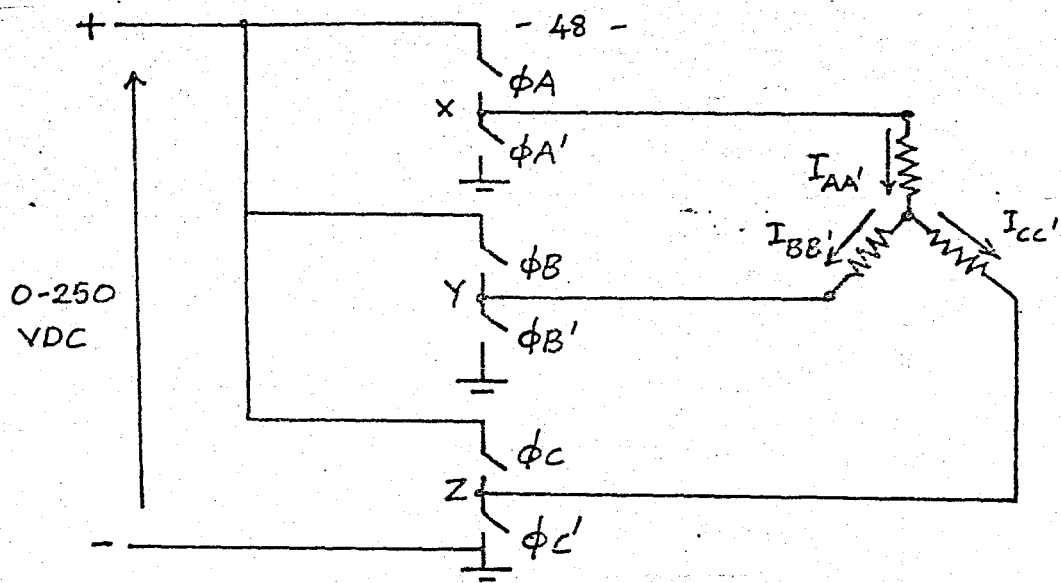


FIGURE 2.12. The Wave-Forms of Darlington Output.

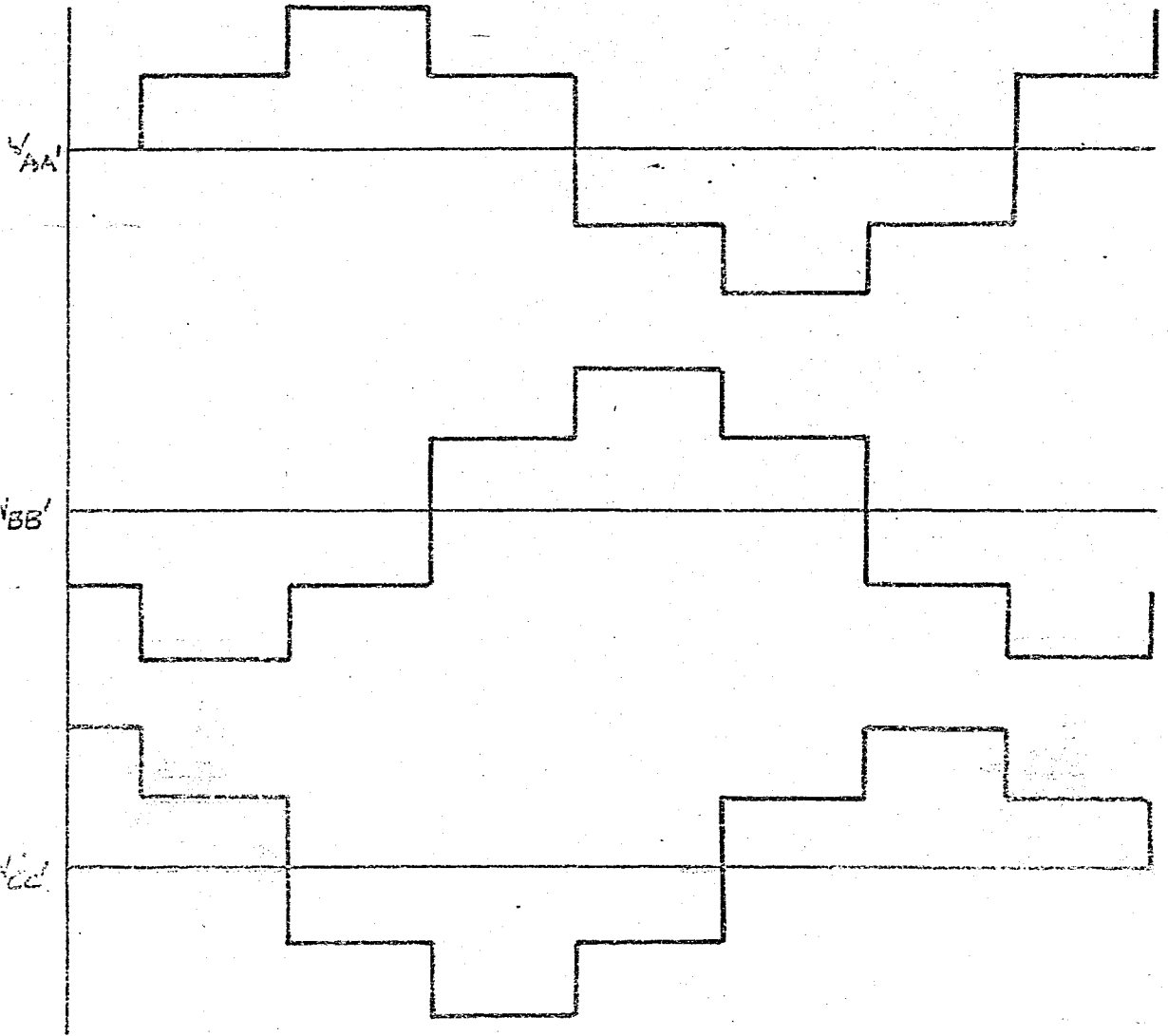


FIGURE 2.13. The Wave Form of the Phase Voltages of the Motor.

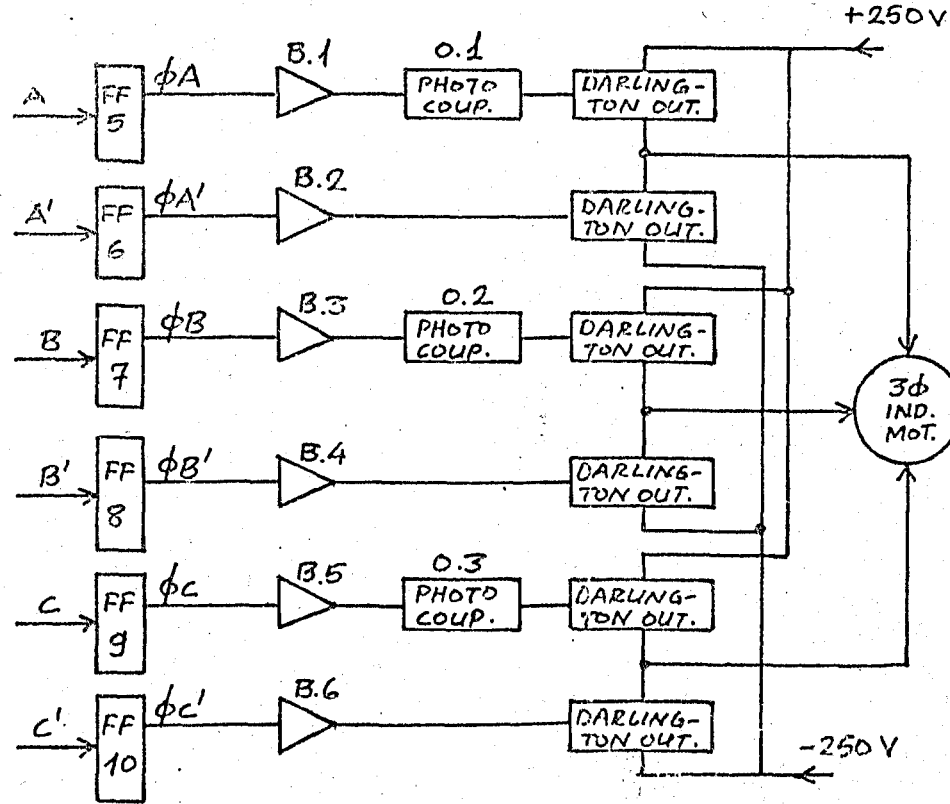


FIGURE 2.14. The Block Diagram of Darlington Output.

CHAPTER 3

A.C. MOTOR OPERATION WITH NON-SINUSOIDAL SUPPLY WAVEFORMS AND VARIABLE-FREQUENCY OPERATION OF INDUCTION MOTORS

Most frequency inverters and static frequency converters generate an output voltage waveform with a significant harmonic content. In this chapter, the motor performance with non sinusoidal supply voltages is compared with normal sine-wave operation.

The most versatile and reliable variable-speed drive consists of a cage-rotor induction motor which is speed-controlled by variation of the stator frequency. The operation of the induction motor on a variable-frequency supply is also examined in this chapter. It will be shown that the presence of harmonics in the supply voltage usually has only a minor influence on the motor performance.

3.1. HARMONIC BEHAVIOR OF A.C. MOTORS

When an a.c. motor is operated on non-sinusoidal supply, the stator voltage can be analysed into a funda-

mental component and a series of harmonics. If magnetic saturation is neglected, the motor may be regarded as a linear device, and the principle of superposition can be applied. This means that the motor behavior can be analysed independently for the fundamental voltage and for each harmonic term. The overall response to the non-sinusoidal voltage is then obtained as a summation of the responses to the individual components. Thus, the net motor current or torque is equal to the sum of the current or torque contributions of each voltage component in the supply waveform. It is convenient to express the motor current and torque in per-unit or normalized form, that is, the actual values of current and torque are expressed as fractions of the rated current and torque of the motor.

Harmonic Equivalent Circuits: The conventional equivalent circuit for one phase of an induction motor on a sinusoidal supply is shown in Figure 3.1a and is derived in Appendix 3. In this circuit, the core losses and saturation effects are neglected, and X_1 and X_2 are the stator and rotor leakage reactances at the supply frequency. X_m is the corresponding magnetizing reactance. The rotor slip with respect to the fundamental rotating field is denoted by S_1 , and hence

$$S_1 = \frac{n_1 - n}{n_1} \quad (3.1)$$

where n_1 is the synchronous speed of the rotating field, and n is the actual rotor speed.

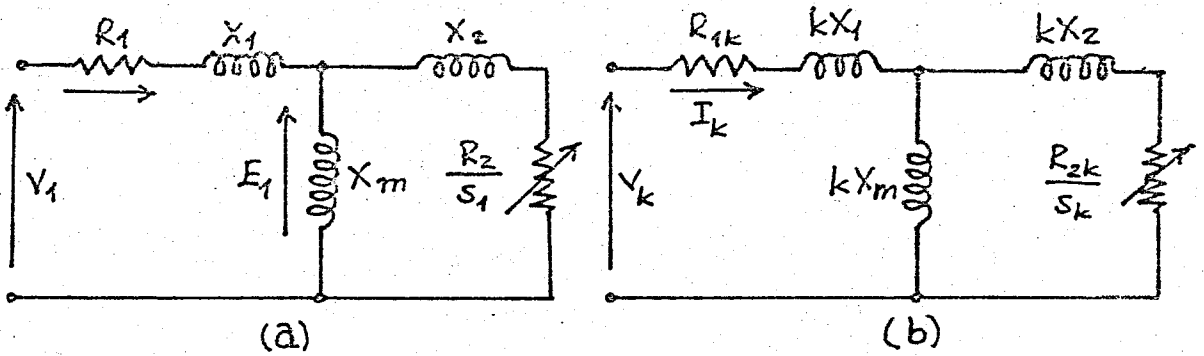


FIGURE 3.1. Induction Motor Equivalent Circuit Diagrams: (a) fundamental-frequency equivalent circuit, (b) equivalent circuit for the k th time harmonic (positive and negative sequence).

The k th harmonic in the phase currents produces a time harmonic m.m.f. rotating forwards or backwards at a speed kn_1 . The rotor slip in a forward-rotating harmonic field is

$$S_k = \frac{kn_1 - n}{kn_1} \quad (3.2)$$

and for a backward-rotating field

$$S_k = \frac{kn_1 + n}{kn_1} \quad (3.3)$$

in general, therefore,

$$S_k = \frac{kn_1 \bar{n}}{kn_1} \quad (3.4)$$

where the negative sign is valid for positive-sequence harmonics and the positive sign applies to negative-sequence harmonics.

The harmonic slip, S_k , is expressed in terms of S_1 by substituting for n from Equation (3.1). This gives

$$S_k = \frac{(k\bar{n} + 1) S_1}{k} \quad (3.5)$$

The fundamental equivalent circuit of Figure 3.1a may be adapted for the k th harmonic voltage and current in Figure 3.1b. The harmonic slip, S_k , is substituted for the fundamental slip, S_1 , and all inductive reactances are increased by a factor k . The stator and rotor resistances are also larger due to skin effect at the harmonic frequency. Strictly speaking, the rotor leakage inductance is also modified by the skin effect, and this must be taken into consideration in precise calculations.

It may be verified by means of Equation (3.5) that there is very little variation in S_k for normal operation. If the motor speed varies from synchronous speed to standstill, the fundamental slip, S_1 , varies from 0 to 1, but

the fifth harmonic slip, S_5 , only varies from 1.2 to 1. The corresponding variation in S_7 is 0.857 to 1, and for higher harmonic S_k is even closer to unity. If we make Fourier Analysis (see Appendix 4) of six-step voltage supply waveform we see that there are no even harmonics because of positive and negative half cycle symmetry, and there are no third or multiples of the third harmonic because of the 60° dwell between the positive and negative waves.

The harmonic equivalent circuit of Figure 3.1b can be simplified as shown in Figure 3.2a by removing the resistances. This is justified by the fact that the inductive reactances increase linearly with frequency, while the increase in rotor resistance with frequency due to skin effect is less than linear. Since S_k is approximately unity, the circuit resistance can be neglected in comparison with the reactance at the harmonic frequencies. Further simplification is possible as in Figure 3.2b, since the shunt magnetizing reactance is much greater than the rotor leakage reactance, and may be omitted. The motor impedance presented to harmonic current is, therefore, approximately $k(X_1 + X_2)$ where X_1 and X_2 are the stator and rotor leakage reactances at the fundamental supply frequency.

The zero-sequence stator current harmonics are in

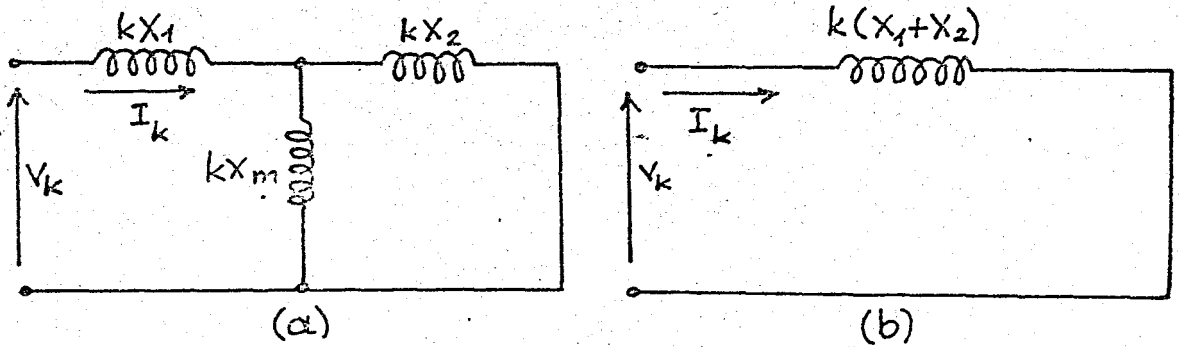


FIGURE 3.2. Approximate Equivalent Circuits for Harmonic Current Calculations.

time phase, and consequently do not produce fundamental rotating m.m.f. wave. However, the zero-sequence currents may establish pulsating space harmonic m.m.f. waves in the air gap, and each pulsating wave can be resolved into a forward and backward-travelling wave, as shown in Table 1. These flux waves induce unequal harmonic currents in the moving rotor, and hence the presence of zero-sequence stator currents can affect the motor torque.

The reactance presented to the flow of the k th zero-sequence harmonic is kX_0 , where X_0 is the stator zero-sequence reactance at fundamental frequency. If X_0 is small and the applied voltage has a large zero-sequence component, the resulting zero-sequence currents may cause a significant stator copper loss, and seriously reduce the motor efficiency. However, zero-sequence currents can only flow in a star-connected system having a neutral connection between source and load, as otherwise there is

TABLE 1

M.M.F. Components of a Three-Phase Armature Winding

Order of space harmonic h	Order of Time Harmonic, k						
	1	3	5	7	9	11	13
1	+1	-	-5	+7	-	-11	+13
3	-	+1	-	-	+3	-	-
5	$-\frac{1}{5}$	-	+1	$-\frac{7}{5}$	-	$+\frac{11}{5}$	$-\frac{13}{5}$
7	$+\frac{1}{7}$	-	$-\frac{5}{7}$	+1	-	$-\frac{11}{7}$	$+\frac{13}{7}$
9	-	$+\frac{1}{3}$	-	-	+1	-	-
11	$-\frac{1}{11}$	-	$+\frac{5}{11}$	$-\frac{7}{11}$	-	+ 1	$-\frac{13}{11}$
13	$+\frac{1}{13}$	-	$-\frac{5}{13}$	$+\frac{7}{13}$	-	$-\frac{11}{13}$	+ 1
15	-	$+\frac{1}{5}$	-	-	$+\frac{3}{5}$	-	-

no return path for the in-phase zero-sequence currents. In practice, most inverter circuits do not generate zero-sequence voltages, but if these components are present they are offered an infinite zero-sequence impedance by isolating the neutral connection.

The fundamental equivalent circuit of Figure 3.1a only applies to the polyphase induction motor, but the subsequent harmonic circuit are also valid for the harmonic behavior of the reluctance or synchronous motor, since these machines operate asynchronously with respect to time harmonic m.m.f. waves. When analysing motor ope-

ration at very low supply frequencies, the approximate harmonic equivalent circuit of Figure 3.2 may not be valid, since the winding resistance can be a significant factor at the low harmonic frequencies. The simplifications are usually justified, however, if the fundamental frequency exceeds about 10 Hz.

Harmonic Currents: Since S_k is nearly unity at all motor speeds from standstill to synchronism, the harmonic equivalent circuit of Figure 3.1b is practically independent of motor speed, and this is emphasized by the approximate circuits derived from it. Thus, the harmonic currents remain constant for all operating conditions of the motor from no-load to full-load, and even down to standstill. The fundamental stator current is determined by the motor loading and, as a result, the relative harmonic content of the machine current is considerably greater for light-load operation than for full-load or starting conditions. This causes a significant increase in the no-load losses of the machine compared with normal sine-wave operation. However, the full-load efficiency is usually not reduced excessively.

The approximate equivalent circuit of Figure 3.2b is similar to that used for normal sine-wave calculations on a locked-rotor induction motor, when the motor current is also limited by the leakage reactance ($X_1 + X_2$). The

standstill or starting behavior of the induction motor on a sine-wave supply is, therefore, a measure of its harmonic performance. If the motor draws a large starting current, it will also draw large harmonic currents on non-sinusoidal supplies. The leakage reactance of a reluctance or synchronous motor also determines its harmonic current flow. If the motor has a very low leakage reactance, it should be used with caution on non-sinusoidal supplies, since excessive harmonic currents may flow and overheat the motor.

If V_k denotes the k th harmonic component of the supply voltage, the corresponding stator current harmonic is $I_k = V_k/Z_k$, where Z_k is the k th harmonic input impedance. For positive- and negative-sequence harmonics, the approximate equivalent circuit of Figure 3.2b is valid, and $Z_k = k(X_1 + X_2)$.

Thus,

$$I_k = \frac{V_k}{k(X_1 + X_2)} \quad (3.6)$$

For zero-sequence harmonics, $Z_k = kX_0$, and

$$I_k = \frac{V_k}{kX_0} \quad (3.7)$$

These formulae permit rapid evaluation of the harmonic currents due to a non-sinusoidal voltage waveform whose harmonic content is known. Usually there are no zero-sequence harmonics and no even numbered harmonics, and hence the total r.m.s. harmonic current is given by

$$I_{\text{har}} = \sqrt{(I_5^2 + I_7^2 + I_{11}^2 + I_{13}^2 + \dots + I_1^2 + \dots)} = \sqrt{\left[\sum_5^{\infty} I_k^2 \right]} \quad (3.8)$$

If I_1 is the fundamental r.m.s. current of the motor, the total r.m.s. stator current, including the fundamental, is

$$I_{\text{r.m.s.}} = \sqrt{(I_1^2 + I_5^2 + I_7^2 + I_{11}^2 + I_{13}^2 + \dots + I_k^2 + \dots)} = \sqrt{[I_1^2 + I_{\text{har}}^2]} \quad (3.9)$$

For a given voltage waveform, the relative harmonic content of the stator current is closely related to the per-unit reactance of the motor, X_{pu} . This is the leakage reactance at fundamental frequency, expressed as a fraction of the base reactance, $X_{\text{base}} = V_R / I_{\text{FL}}$, where V_R is the rated sine-wave phase voltage, and I_{FL} is the rated full-load current.

Thus,

$$X_{pu} = \frac{(X_1 + X_2)}{X_{base}} = (X_1 + X_2) \cdot \frac{I_{FL}}{V_R} = \frac{I_{FL}}{I_S} \sin \phi_s \quad (3.10)$$

where I_S is the fundamental standstill current of the motor and ϕ_s is the motor power factor angle at standstill.

For the usual six-step and twelve-step voltage waveforms, the magnitude of the harmonic voltage is inversely proportional to the order of the harmonic. Thus $V_k = V_1/k$, and Equation (3.6) gives the harmonic current

$$I_k = \frac{V_k}{k^2 (X_1 + X_2)} \quad (3.11)$$

If the fundamental phase voltage, V_1 , is equal to the rated sine-wave voltage, V_R , then Equation (3.10) gives

$$V_1 = V_R = (X_1 + X_2) \frac{I_{FL}}{X_{pu}}$$

and substituting this expression in (3.11) gives

$$I_{kpu} = \frac{I_k}{I_{FL}} = \frac{1}{k^2 X_{pu}} \quad (3.12)$$

where I_{kpu} is the per-unit harmonic current on the rated

full load current.

Using Equations (3.8) and (3.12), the total r.m.s. per-unit harmonic current with a six-step voltage supply is evaluated as $0.046/X_{pu}$. Similar calculations on a twelve-step supply give a value of $0.0105/X_{pu}$. Thus the harmonic current is inversely proportional to the per-unit reactance. The total r.m.s. stator current at full-load on a per-unit basis is $\sqrt{[1+(0.046/X_{pu})^2]}$ for a six-step voltage waveform and $\sqrt{[1+(0.0105/X_{pu})^2]}$ with a twelve-step supply. In Figure 3.3, the total r.m.s. stator current is plotted as a function of the per-unit reactance. The increase in r.m.s. current is almost negligible with a twelve-step supply but the six-step voltage waveform can produce a significant increase, particularly when the per-unit reactance is small. This occurs principally with reluctance motors which may have a per-unit reactance as low as 0.05, resulting in a 35 percent increase in the r.m.s. full load current. The polyphase induction motor has a per-unit reactance in the range 0.1 to 0.2, and the total r.m.s. current at full-load on a six-step voltage supply is from 2 to 10 percent greater than fundamental current.

Figure 3.4a shows a typical stator phase current waveform for an a.c. motor with a six-step voltage supply. This waveform was calculated for a per-unit of 0.1, as-

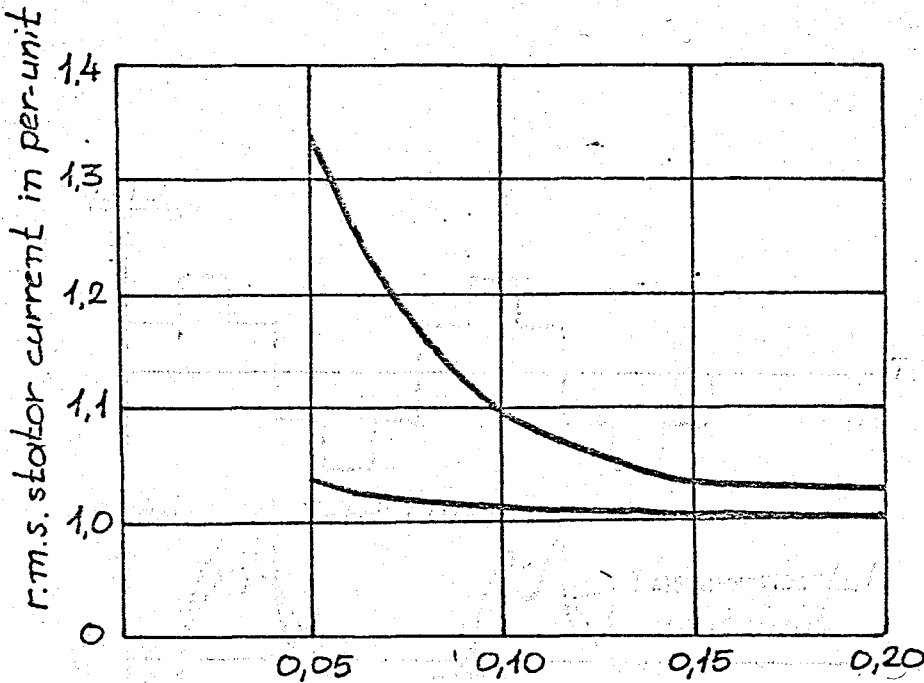


FIGURE 3.3. R.M.S. Stator Current as a Function of the Per-Unit Leakage Reactance of the Motor.

suming that the fundamental current lags the fundamental voltage by 60° . This fundamental phase angle is determined by the loading conditions and, in the present case, it corresponds to a fundamental power factor of 0.5. The corresponding current waveform with a twelve-step supply is shown in Figure 3.4b. The harmonic distortion not only increases the r.m.s. value of the stator current, but also produces large current peaks which increase the commutating duty imposed on the static inverter. In Figure 3.5 the ratio of the peak inverter current to the peak fundamental full-load current is plotted as a function of the per-unit reactance. These characteristics were derived theoretically, assuming a fundamental power factor or displacement factor of 0.5. With lower displacement factors,

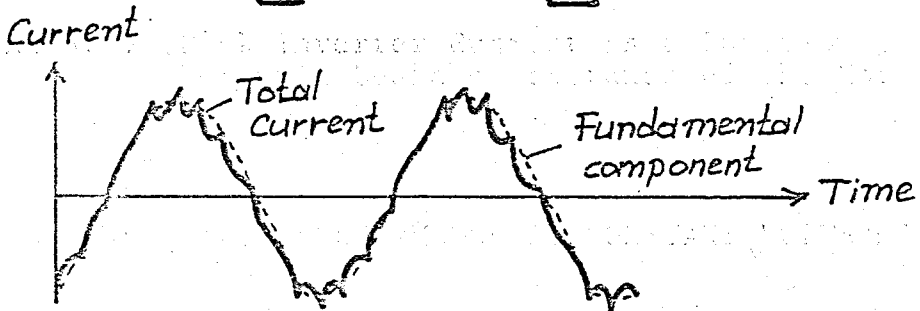
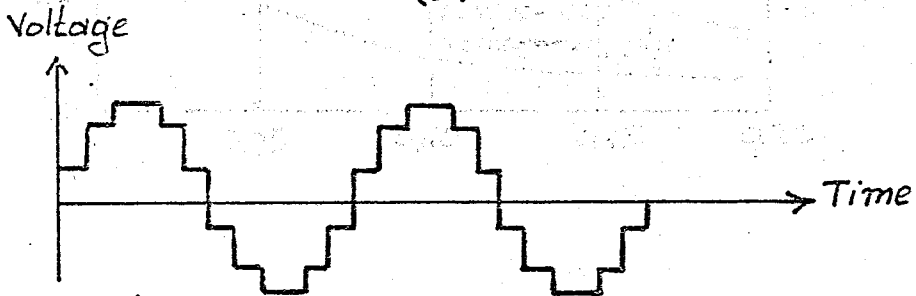
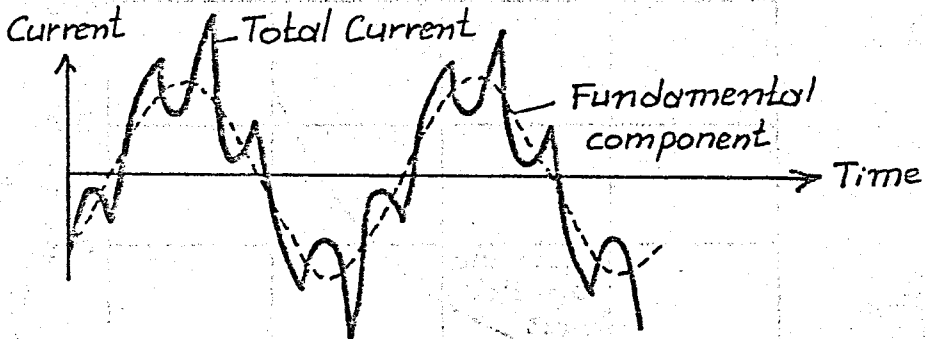
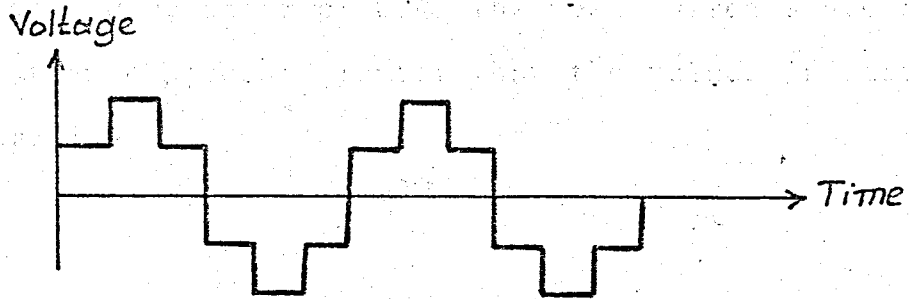


FIGURE 3.4. (a) Stator Voltage and current waveforms for a.c. Motor with a Six-step Voltage Supply, (b) Stator voltage and current waveforms for a.c. motor with a twelve-step voltage supply.

the peak inverter currents are somewhat larger. For an a.c. motor operating on a six-step supply with a fundamental power factor of 0.4, the peak currents are not more than 4 percent greater than the values indicated in Figure 3.5.

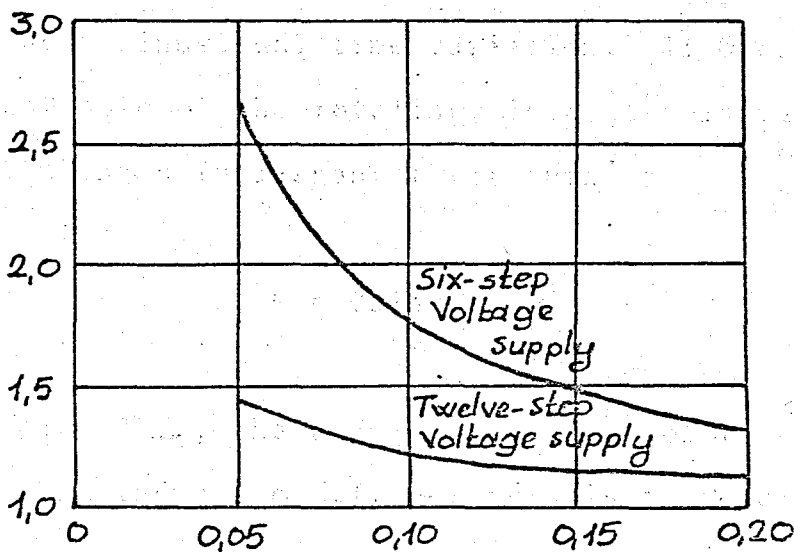


FIGURE 3.5. Peak Inverter Current as a Function of the Per-unit Leakage Reactance of the Motor.

3.2. STEADY-STATE PERFORMANCE AT CONSTANT VOLTS/HZ

The steady-state performance of the induction motor is readily analysed by means of the fundamental equivalent circuit of Figure 3.1a. For normal sine-wave operation, the skin effect is usually neglected, and hence the resistances are independent of frequency, while the reactances

are proportional to frequency. The rotating flux wave in the air gap induces a counter e.m.f. E_1 in the stator winding. This e.m.f. is less than the applied voltage V_1 due to the voltage drop in $(R_1 + jX_1)$, the stator leakage impedance. Since the presence of space harmonic m.m.f. waves is ignored, the rotating flux wave has a sinusoidal space distribution, and the flux linking each stator turn has a sinusoidal time variation. If ϕ denotes the flux per pole of the rotating field, the instantaneous flux linking a full-span stator turn is

$$\phi = \phi_m \sin \omega_1 t$$

where $\omega_1 = 2\pi f_1$, the angular frequency of the supply voltage. The induced e.m.f. per turn is therefore

$$e_1 = d\phi/dt = \omega_1 \phi_m \cos \omega_1 t$$

and the r.m.s. phase e.m.f. is given by

$$E_1 = \omega_1 \phi_m k_w N_1 / \sqrt{2} = 4.44 k_w f_1 N_1 \phi_m \quad (3.13)$$

where N_1 is the number of series turns per phase and k_w is the winding factor. If the winding factor is unity, the usual transformer e.m.f. equation is obtained and, hence, for a motor or transformer, ϕ_m is proportional to E_1/f_1 .

For effective utilization, the air-gap flux of the induction motor must be sustained at all frequencies. A constant air gap flux is obtained when the ratio E_1/f_1 is constant, but if the stator leakage impedance is small, then V_1 and E_1 are approximately equal. Consequently, the air-gap flux is nearly constant when the ratio V_1/f_1 has a fixed value. This is the constant volt/Hz mode of operation. The linear output voltage-frequency characteristic is provided by the static inverter or cycloconverter, using the voltage control techniques. Unfortunately, the motor performance deteriorates at low frequencies when the air-gap flux decreases. This is shown in the following section.

Torque Characteristics: From the equivalent circuit of Figure 3.1a, the following phasor equations may be obtained:

$$V_1 = (R_1 + jX_1)I_1 + \left(\frac{R_2}{s} + jX_2\right)I_2 \quad (3.14)$$

$$jX_m(I_1 - I_2) = \left(\frac{R_2}{s} + jX_2\right)I_2 \quad (3.15)$$

By definition, the rotor slip is given by

$$s = f_2/f_1 \quad (3.16)$$

where f_1 is the variable stator frequency, and f_2 is the

corresponding rotor frequency.

In Appendix 3, the motor torque is derived as

$$T = \frac{pm_1}{2\pi f_1} I_2^2 \frac{R_2}{s} \quad (3.17)$$

where m_1 is the number of stator phases, and p is the number of pole-pairs.

On combining Equations (3.14), (3.15) and (3.17), the torque can be expressed in terms of the applied voltage V_1 and the frequencies f_1 and f_2 . The resulting expression is

$$T = \frac{pm_1}{2\pi} \left[\frac{V_1}{f_1} \right]^2 \frac{f_2 X_m^2 / R_2}{\left[R_1 + \frac{f_2}{f_1 R_2} (X_m^2 - X_{11} X_{22}) \right]^2 + \left[X_{11} + \frac{f_2 R_1 X_{22}}{f_1 R_2} \right]^2} \quad (3.18)$$

where $X_{11} = X_1 + X_m$, the total stator reactance at the supply frequency f_1 , and $X_{22} = X_2 + X_m$, the total rotor reactance at the same frequency.

For fixed volts/Hz operation, the quantity V_1/f_1 in Equation (3.18) is constant, and the torque characteristics can be evaluated when the machine parameters are known. In Figure 3.6 the torque is plotted against rotor frequency, f_2 , for a number of stator frequencies. The

torque is again expressed in per-unit form, using the rated torque of the motor as a base value. These results show that the induction motor torque decreases rapidly as the stator frequency is reduced. This is caused by the reduction in air-gap flux at low frequency due to the increased influence of the stator resistance. The stator resistance voltage drop at rated current has the same magnitude at all frequencies, and it therefore constitutes a considerably higher fraction of the supply voltage at low frequency than at rated frequency, when it may often be neglected.

The torque characteristics may be extended into the induction generator region as in Figure 3.6. In this

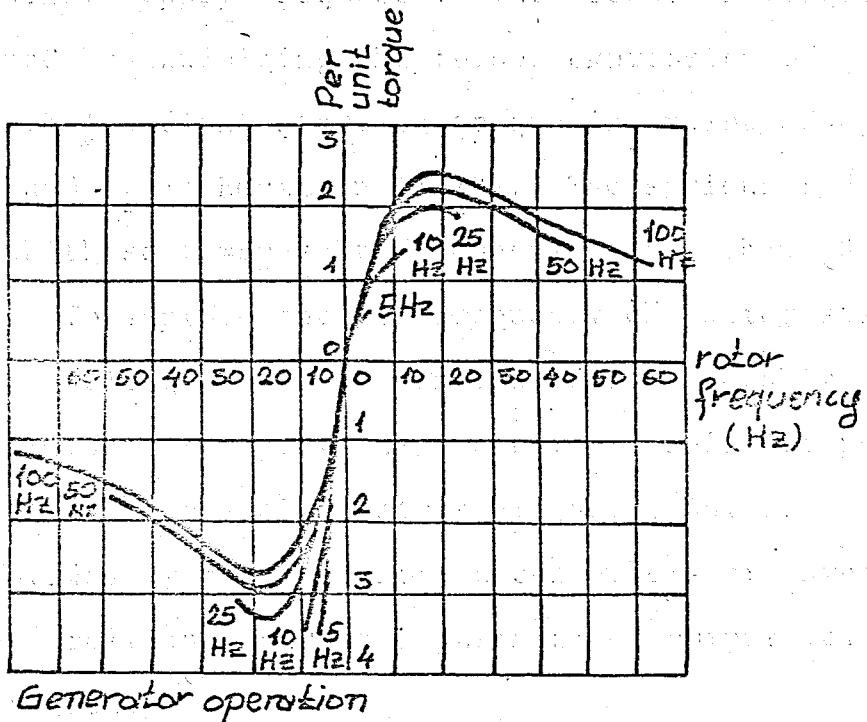


FIGURE 3.6. Torque Characteristics for Variable-Frequency Operation of the Induction Motor at Constant Volts/Hz.

region, the machine operates with a reversed power flow and reversed stator voltage drop, resulting in increased e.m.f. E_1 , and increased air-gap flux. Consequently, large generator torques are produced, particularly at low frequencies. These braking torques may cause mechanical damage, unless current limiting is employed. However, the characteristics of Figure 3.6 are based on the linear equivalent circuit of Figure 3.1a, in which magnetic saturation is neglected. In practice, saturation effects will cause the braking torques in the generator region to be less than the theoretical values indicated in Figure 3.6.

In Figure 3.7 the breakdown and starting torques are plotted against supply frequency. The breakdown torque is determined by maximizing the torque expression of Equation (3.18) and the starting torque is evaluated by putting f_1 and f_2 in Equation (3.18). The serious reduction in both these torques at frequencies less than 10 Hz is evident. To improve the low-frequency characteristics, the terminal voltage should be increased considerably above its frequency-proportional value. This is not possible when synchronous alternators are used, but is readily provided by means of static converters or inverters which permit independent adjustment of output voltage and frequency.

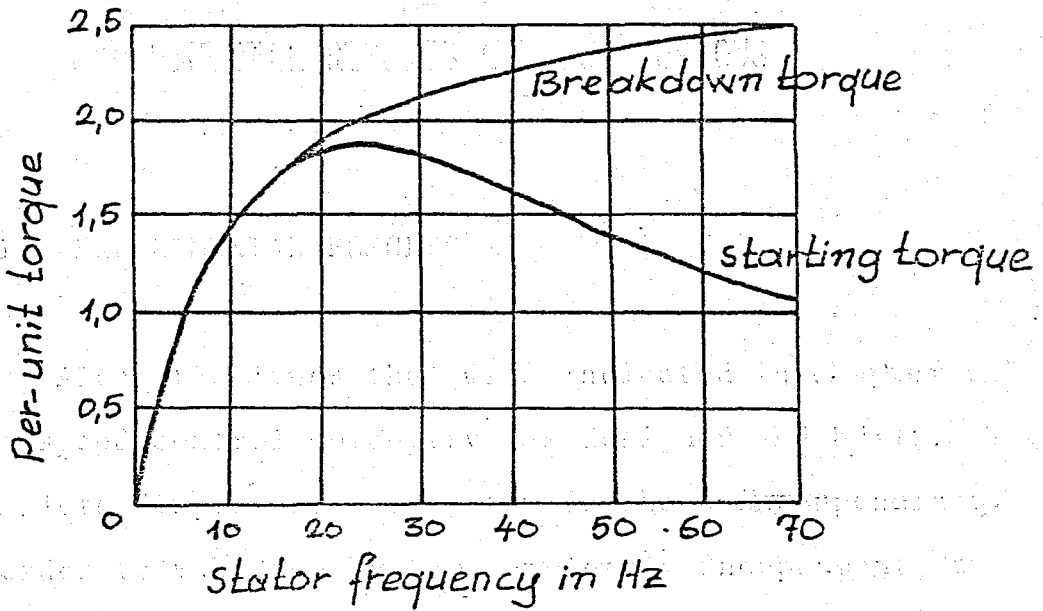


FIGURE 3.7. Starting and Breakdown Torques for Variable-Frequency Operation of the Induction Motor at Constant Volts/Hz.

CHAPTER 4

EXPERIMENTAL RESULTS AND CONCLUSIONS

4.1. EXPERIMENTAL RESULTS

Along the lines that were indicated in Chapter 2, the speed control circuitry was designed and built. The complete diagram of the system is shown in Appendix 6. In order to make the system completely independent, a single phase bridge rectifier was included in the input to provide the d.c. voltage.

The system was tested on different induction machines and it was seen that smooth control of speed was possible. The highest operating frequency had to be limited to 10 Hz due to the rating of the Darlington transistors used.

The relation between input voltage and the output frequency is shown in Figure 4.1. It can be seen that it is a linear relationship as expected. The same linearity of the U.J.T. output was checked up to 400 volts corresponding to 90 Hz.

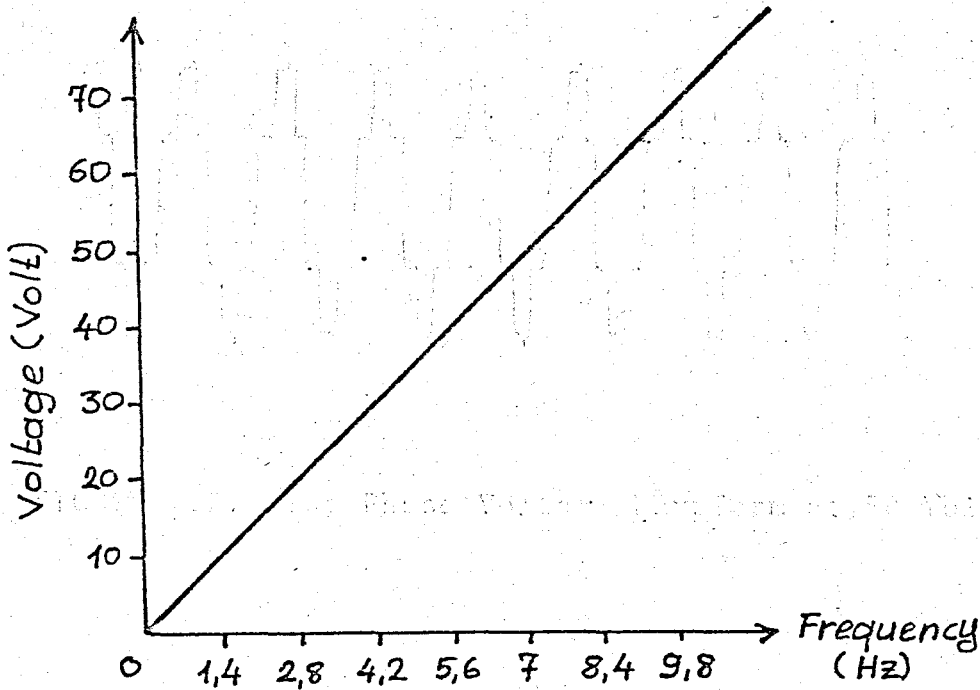


FIGURE 4.1. The Input Voltage to Output Frequency Characteristic.

Figures 4.2, 4.3, 4.4, 4.5 and 4.6 show typical waveforms of phase voltage and phase current for 70V and 40 V inputs. As can be seen, these are the same as the theoretical waveforms shown in Figure 3.4a and b.

Figure 4.7 shows the speed output as a function of input voltage.

It is observed that at low values of input voltage the machine is not able to pick up speed. This is to be expected from Figure 3.7, from which it can be seen that the starting torque is considerably reduced at low supply

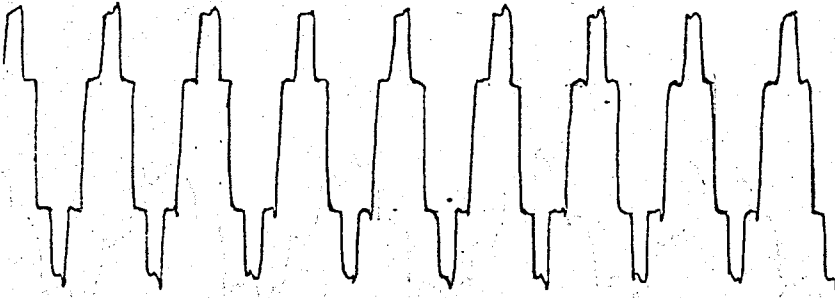


FIGURE 4.2. The Phase Voltage Waveform at 70 Volts.

FIGURE 4.3. The Phase Current Waveform at 70 Volts.

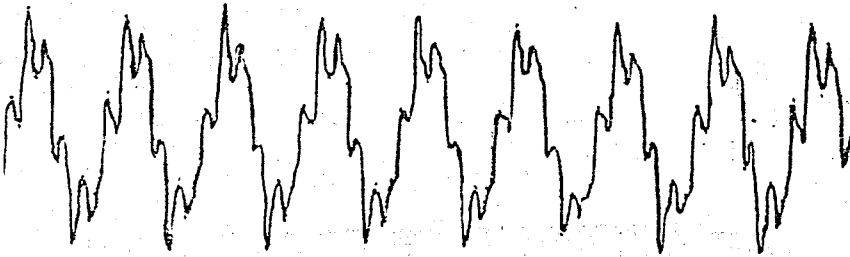


FIGURE 4.3. The Phase Current Waveform at 70 Volts.



FIGURE 4.4. The Phase Voltage Waveform at 40 Volts.



FIGURE 4.5. The Phase Current Waveform at 40 Volts.

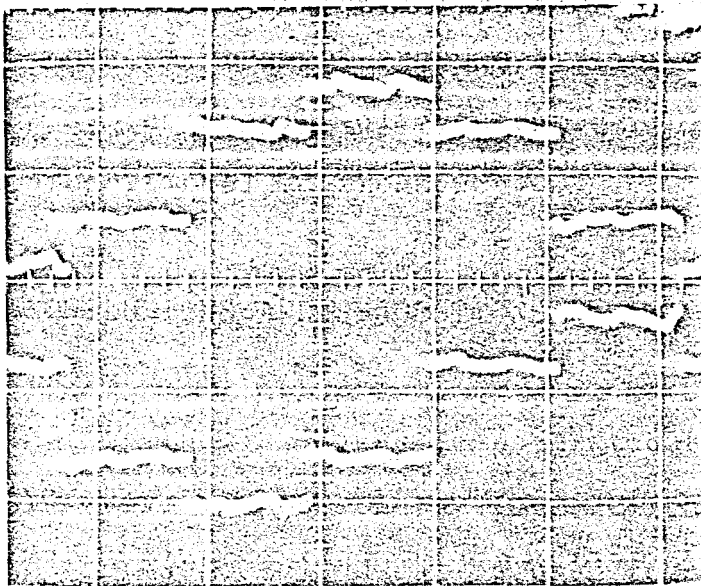


FIGURE 4.6. The Waveforms of Phase Voltage V_{AA} , and V_{BB} .

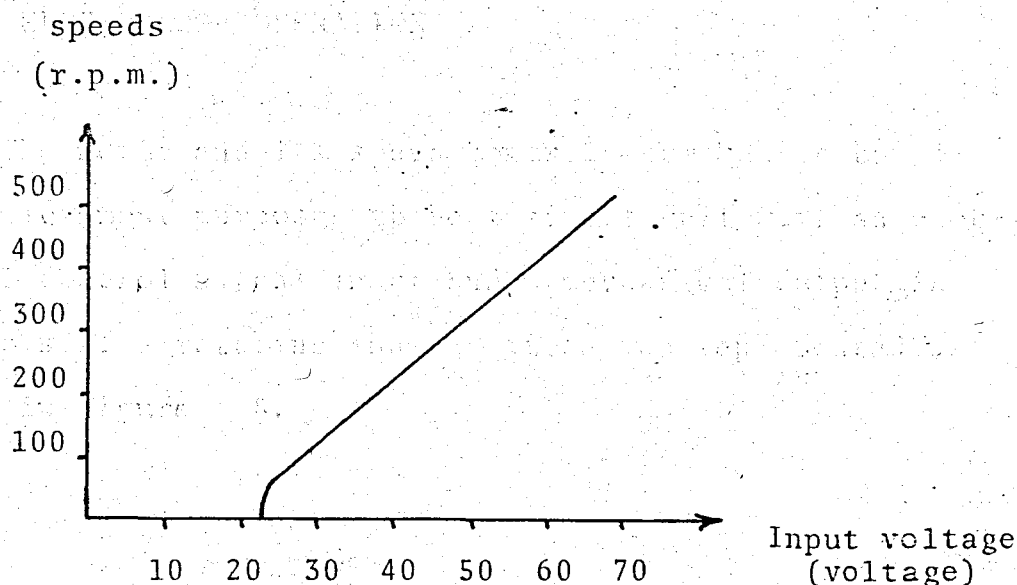


FIGURE 4.7. The Input Voltage to the Speed Output Characteristics.

frequencies. As was suggested before, this problem can be overcome, if the low speed operation is a must, by increasing the supply voltage considerably above its value proportional to frequency.

4.2. CONCLUSIONS AND SUGGESTIONS

In this thesis it was demonstrated that the synthesis of a sine-wave is possible by logic circuit. The three-phase output so obtained can be used to smoothly control the speed of an induction machine in a 10-1 range.

If a closed loop operation is desired, it can be achieved with minor modifications as explained below.

4.3. CLOSED-LOOP OPERATION

The motor and its speed control gear can be considered for most purposes to be a single unit with an electrical control signal input and a mechanical output in the form of a rotating shaft. It can be represented as shown in Figure 4.8.

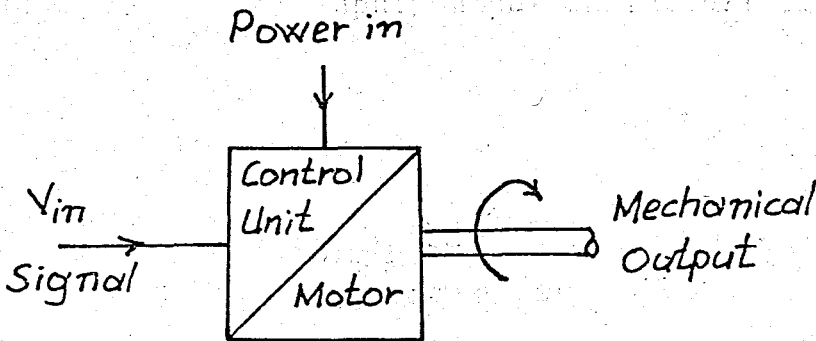


FIGURE 4.8. Basic Control System.

The input to output characteristic is ideally as that shown in Figure 4.9. However, owing to loading on the motor, the motor speed will decrease with increased load.

In order to be able to keep V/f a constant, a controllable rectifier should be used at the input, the error voltage acting on the firing angle of the bridge converter. Figure 4.10 shows a possible realization.

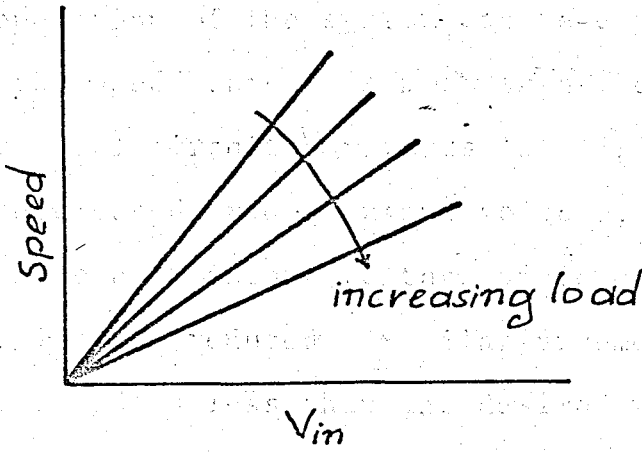


FIGURE 4.9. Ideal Input/Output Characteristic of Figure 4.8.

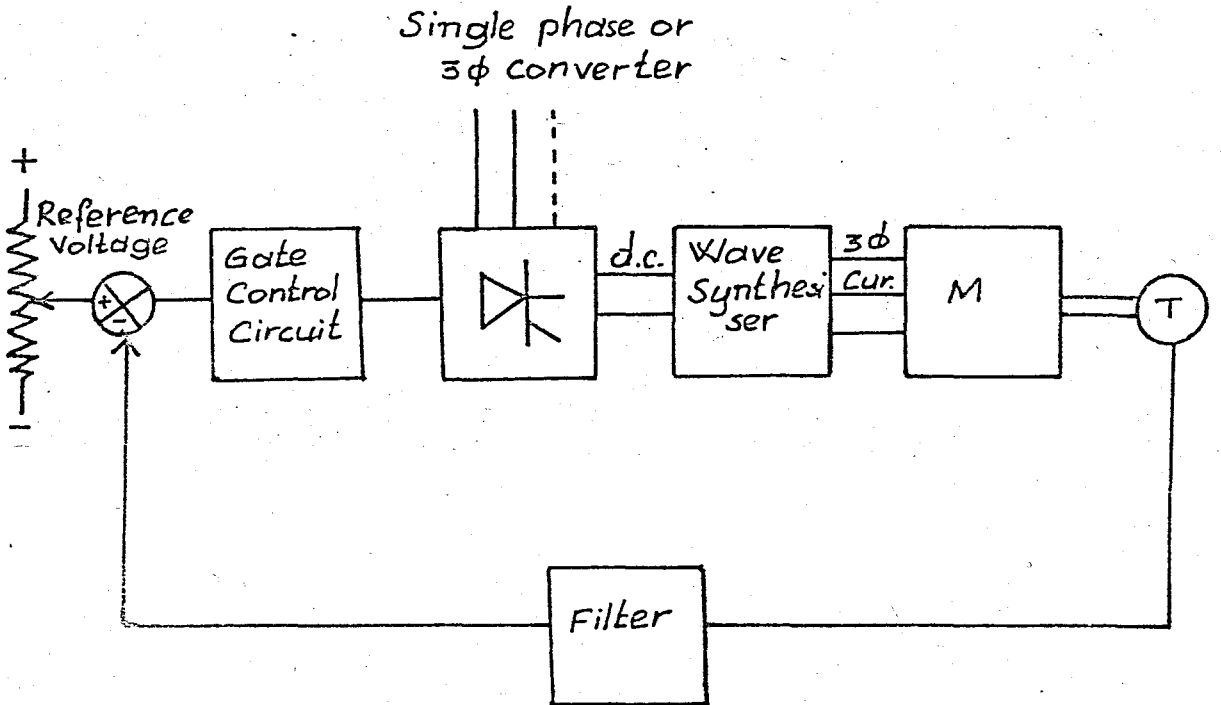


FIGURE 4.10. Basic Control System with Error Feedback.

The operation of the system can be explained as follows: If the speed output is more than the set value, the gate control circuitry retards the firing angle to result in decreased bridge output voltage, which is then converted into a 3 ϕ output voltage of lower frequency. The output is thus reduced. Similar argument holds if the output speed is less than the desired value.

REFERENCES

1. Irving M. Gottlieb: Principles and Applications of Inverters and Converters, 1977.
2. Irving M. Gottlieb: Electric Motors and Electronic Motor Control Techniques, 1976.
3. R.S. Ramshaw: Power Electronics, Thyristor Controlled Power Electric Motors, 1978.
4. J.M.D. Murphy: Thyristor Control of A.C. Motors, 1978.
5. E.H. Werninck: Electric Motor Handbook, 1978.
6. Noel Morris: Industrial Electronics, 1978.
7. Noel Morris: Advanced Industrial Electronics, 1974.
8. Thomas C. Barte: Digital Computer Fundamentals, 1977.
9. Power Semiconductor Applications, IEEE Press, Vol. I and II, 1972.
10. C.S. Siskind: Electrical Machines, 1959.
11. J.Schaefer, Wiley: Rectifier Circuit, 1964.
12. David J. Comer: Modern Electronic Circuit Design, 1976.
13. Millman-Halkias: Integrated Electronics, 1972.
14. P. Bowler: Power Transistors in Variable Speed Drives. Electronic and Power, Vol. 24, October 1978, pp. 730-736.
15. A.R.W. Broadway: Multispeed Induction Motor Fed From a Switched Single-Phase Supply, Proc. IEE, Vol. 125, May 1978, pp. 400-406.
16. M.H. Nehrir: Speed Control of Three-Phase Induction Motor by Stator Voltage Control, IEEE Trans., Vol. IECI-22, May 1975.
17. M.Ray and A.K. Datta: A Variable-Speed Induction Motor Using Thyristor Chopper, IEE Proceed., Vol. 121, October 1974.

APPENDIX 1

MEASUREMENTS OF THE COMPONENTS V.C.O.

$$\text{Chosen: } R = R_1 + R_2 = 220 + 110 = 330 \text{ k}\Omega$$

$$R_1 = 560 \text{ }\Omega$$

$$R_2 = 220 \text{ }\Omega$$

220 \rightarrow 50 Hz, 30 V \rightarrow 7 Hz then;

f must be 7 Hz for 30 V, then; $f = 7 \times 24 = 168 \text{ Hz}$ for U.J.T.

($f = 168 \text{ Hz}$ for 30V, $f = 1200 \text{ Hz}$ for 220V in V.C.O.)

$$t = \frac{1}{f} = \frac{1}{168} = 0.005952381 \text{ s}$$

30 V \rightarrow 0,005952381 s; 12 V \rightarrow 0,0148807 s; $\eta = 0.55$

$$t = 0.8RC \text{ (R = k}\Omega \text{ , t:s, C:F)}$$


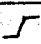
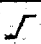
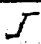

$$C = \frac{t}{0.8R} = \frac{0.0148807}{0.8 \cdot 330} = 0.0000563 \text{ F}$$

$$C = 0.05 \text{ }\mu\text{F}$$

APPENDIX 2




TRUTH TABLES OF J-K AND D TYPE FLIP-FLOPS

Truth Table of J-K Type Flip-Flop

Inputs						Outputs*	
C^{\dagger}	J	K	S	R	$Q_n^{\#}$	Q_{n+1}	\bar{Q}_{n+1}
	1	X	0	0	0	1	0
	X	0	0	0	1	1	0
	0	X	0	0	0	0	1
	X	1	0	0	1	0	1
	X	X	0	0	X	Q_n	\bar{Q}_n
X	X	X	1	0	X	1	0
X	X	X	0	1	X	0	1
X	X	X	1	1	X	1	1

No change

Truth Table of D Type Flip-Flop

Inputs				Outputs	
Clock [†]	Data	Reset	Set	Q	\bar{Q}
	0	0	0	0	1
	1	0	0	1	0
	X	0	0	Q	\bar{Q}
X	X	1	0	0	1
X	X	0	1	1	0
X	X	1	1	1	1

No change

X = Don't Care

† = Level Change

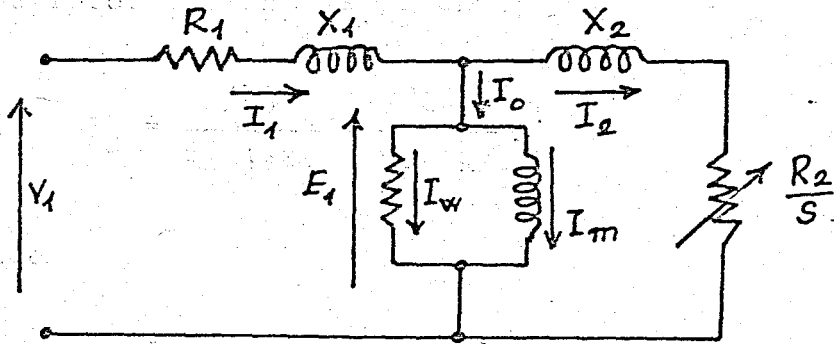
= Present State

* = Next State

APPENDIX 3

EQUIVALENT DIAGRAM OF THE POLYPHASE INDUCTION MOTOR

The equivalent circuit of the induction motor is very similar to the usual transformer equivalent circuit, since the induction motor is essentially a transformer with a rotating secondary winding. As in a static transformer, the primary or stator current establishes a mutual flux which links the secondary or rotor winding, and also a leakage flux which links only the primary winding. This leakage flux induces a primary e.m.f. which is proportional to the rate of change of primary current, and its effect may be represented, in the usual manner, by a series leakage reactance X_1 in each stator phase. R_1 is the stator resistance per phase and $(R_1 + jX_1)$ is termed the stator leakage impedance. The mutual flux in the air gap induces slip frequency e.m.f.s in the rotor and supply frequency e.m.f.s in the stator. The voltage drop across the stator leakage impedance causes the stator e.m.f. per phase, E_1 , and mutual flux per pole, ϕ , to decrease slightly as load is applied to the motor. The resultant stator current I_1 is composed of the exciting current, and the load component of the stator current which cancel



Single-Phase Equivalent Circuit of the Polyphase Induction Motor.

the m.m.f. due to the rotor current. The exciting current I_0 consists of the magnetizing and core-loss components, I_m and I_w respectively.

In deriving the rotor equivalent circuit, the actual phase-wound or squirrel-cage rotor winding is considered to be replaced by an equivalent short-circuited rotor winding having the same number of turns and the same winding arrangement as the stator. This is equivalent to the usual transformer procedure of referring secondary quantities to the primary. At standstill, the induced e.m.f. per phase in the equivalent rotor is equal to the stator e.m.f., E_1 , and the rotor frequency equals the supply frequency, f_1 . When the motor runs with a slip s , the rotor e.m.f. $E_2 = sE_1$, and the rotor frequency $f_2 = sf_1$. If R_2 is the equivalent rotor resistance per phase, and X_2 is the rotor leakage reactance per phase at standstill,

then the rotor current is given by

$$I_2 = \frac{E_2}{R_2 + jsX_2} = \frac{sE_1}{R_2 + jsX_2} \quad (\text{A.3.1})$$

and hence

$$I_2 = \frac{E_1}{(R_2/s) + jX_2} \quad (\text{A.3.2})$$

In Equation (A.3.1), all rotor quantities are at slip frequency, but in Equation (A.3.2) they are at supply frequency. This shows that the rotor current I_2 is unaltered in magnitude if the rotor is brought to standstill and the resistance increased from R_2 to R_2/s . The rotor equivalent circuit may therefore be joined directly to the stator circuit, as in Figure , to give the complete equivalent circuit for one phase of the motor.

Torque Equation: At a slip s , the rotor loss in the equivalent circuit is $I_2^2 R_2/s$ watts per phase, whereas in the actual machine the rotor copper loss is $I_2^2 R_2$ watts per phase. The additional power loss in the equivalent circuit is the electrical equivalent of the mechanical power output of the motor. If P_{mech} denotes the gross mechanical power output including windage and friction losses, then

$$P_{\text{mech}} = m_1 [(I_2^2 R_2/s) - (I_2^2 R_2)] = m_1 I_2^2 R_2 \left(\frac{1-s}{s}\right)$$

where m_1 is the number of stator phases.

If ω is the mechanical angular velocity of the rotor and T is the electromagnetic torque

$$T_\omega = m_1 I_2^2 R_2 \left(\frac{1-s}{s}\right)$$

and

$$T = \frac{m_1 I_2^2 R_2}{\omega} \left(\frac{1-s}{s}\right)$$

This is the internal motor torque which is greater than the useful shaft torque by the amount required to overcome the windage and friction torques.

Since the synchronous angular velocity is given by $\omega_1 = \omega/(1-s) = 2\pi f_1/p$, the torque equation can be rewritten as

$$T = \frac{m_1 I_2^2 R_2}{s\omega_1} \quad (\text{A.3.3})$$

or

$$T = \frac{pm_1}{2\pi f_1} (I_2)^2 \frac{R_2}{s} \quad (\text{A.3.4})$$

Power Division in the Rotor: It can be seen from the equivalent circuit that the total electrical power input to the rotor across the air-gap from the stator is

$$P_{ag} = m_1 I_2^2 R_2 / s \quad (A.3.5)$$

This is divided between the mechanical power output, P_{mech} , and the rotor copper loss, P_2 .

Thus,

$$P_{ag} = P_{mech} + P_2$$

where

$$P_{mech} = T\omega$$

and

$$P_2 = m_1 I_2^2 R_2$$

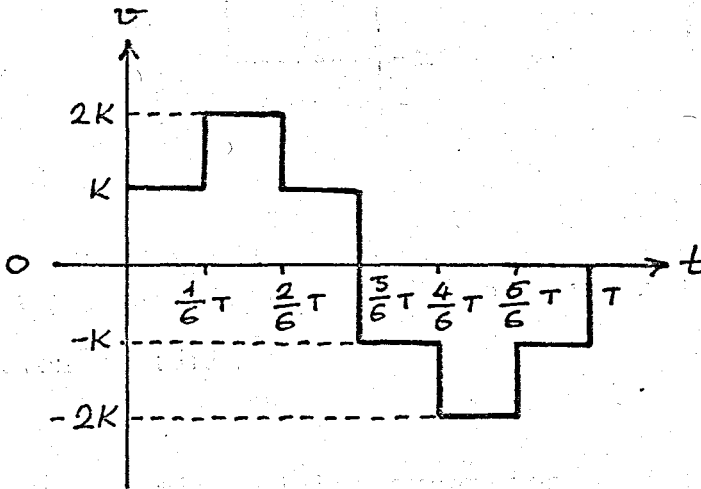
Combining Equations (A.3.4) and (A.3.5) gives

$$P_{ag} = T\omega_1 \quad (A.3.6)$$

and hence the total electrical power input to the rotor is equal to the internal mechanical torque multiplied by the synchronous angular velocity.

APPENDIX 4

FOURIER ANALYSIS OF NON-SINUSOIDAL WAVEFORM



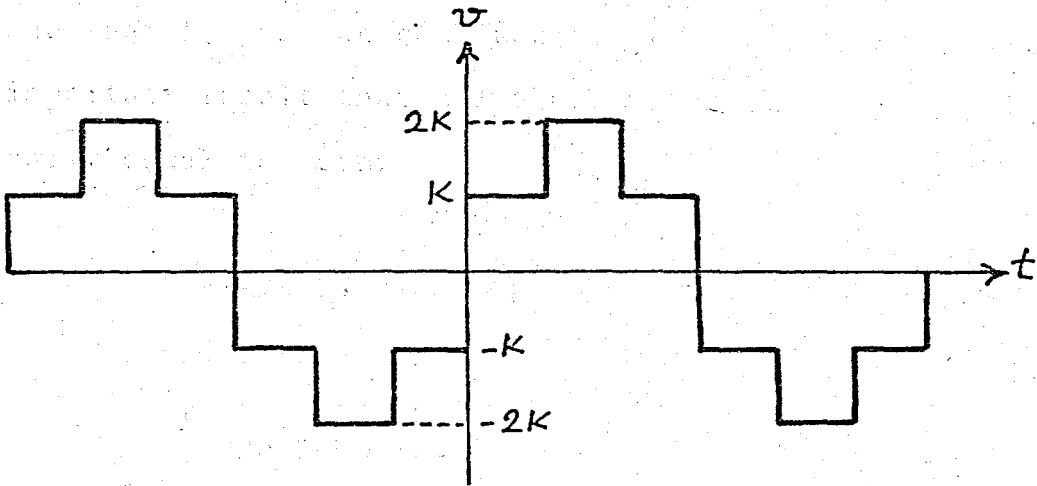
$$v(t) = Ku(t) + Ku(t - \frac{1}{6}T) - Ku(t - \frac{2}{6}T) - 2Ku(t - \frac{3}{6}T) - Ku(t - \frac{4}{6}T) + Ku(t - \frac{5}{6}T) + Ku(t - T)$$

where in the above equation $Ku(t - \tau)$ is defined as:

$$Ku(t - \tau) = \begin{cases} K & t \geq \tau \\ 0 & t < \tau \end{cases}$$

Let F denote the periodic extension of v to the entire X

axis.



From the above figure it is obvious that F is an odd function of time.

The Fourier series expansion of the function $v(t)$ will be of the form:

$$v(t) = \frac{a_0}{2} + \sum_{n=1}^{\infty} \left[a_n \cdot \cos\left(\frac{2n\omega t}{T}\right) + b_n \cdot \sin\left(\frac{2n\omega t}{T}\right) \right]$$

where

$$a_k = \frac{2}{T} \int_0^T v(t) \cos(n t) dt$$

and

$$b_k = \frac{2}{T} \int_0^T v(t) \sin(n t) dt$$

Using the fact that:

$$\int_0^T F(t) \cos(n\omega t) dt = \int_0^T v(t) \cos(n\omega t) dt$$

and that $F(t)$ is an odd function of time; we conclude the important result that all the a_n coefficients are identically equal to zero.

$$F(t) \cdot \cos(n\omega t) = \text{ODD FUNCTION}$$

$$(\text{odd}) \cdot (\text{even})$$

$$\int_0^T \text{ODD FUNCTION} \cdot dt = 0$$

Therefore it is only necessary to compute the b_n coefficients:

$$b_n = \frac{2}{T} \int_0^T v(t) \sin\left(\frac{2n\pi}{T} \cdot t\right) dt$$

$$b_n = \frac{2}{T} \left[\int_0^T K \sin\left(\frac{2n\pi}{T} \cdot t\right) dt + \int_{\frac{1}{6}T}^T K \sin\left(\frac{2n\pi}{T} \cdot t\right) dt \right]$$

$$- \int_{\frac{2}{6}T}^T K \sin\left(\frac{2n\pi}{T} t\right) dt - \int_{\frac{3}{6}T}^T 2K \sin\left(\frac{2n\pi}{T} t\right) dt$$

$$- \int_{\frac{4}{6}T}^T K \sin\left(\frac{2n\pi}{T} t\right) dt + \int_{\frac{5}{6}T}^T K \sin\left(\frac{2n\pi}{T} t\right) dt$$

$$+ \int_{\frac{1}{6}T}^T K \sin\left(\frac{2n\pi}{T} t\right) dt$$

G

$$A = \int_0^T K \sin\left(\frac{2n\pi}{T} \cdot t\right) dt = -\frac{KT}{2n\pi} \cos\left(\frac{2n\pi}{T}t\right) \Big|_0^T$$

$$= -\frac{KT}{2n\pi} (\cos 2n\pi - \cos 0^\circ) = 0$$

$$B = \int_{\frac{1}{6}T}^T K \sin\left(\frac{2n\pi}{T}t\right) dt = -\frac{KT}{2n\pi} \cos\left(\frac{2n\pi}{T}t\right) \Big|_{\frac{1}{6}T}^T$$

$$= -\frac{KT}{2n\pi} (\cos 2n\pi - \cos \frac{n\pi}{3})$$

$$= -\frac{KT}{2n\pi} (1 - \cos \frac{n\pi}{3})$$

$$C = -\int_{\frac{2}{6}T}^T K \sin\left(\frac{2n\pi}{T}t\right) dt = \frac{KT}{2n\pi} (1 - \cos \frac{2n\pi}{3})$$

$$D = -\int_{\frac{3}{6}T}^T 2K \sin\left(\frac{2n\pi}{T}t\right) dt = \frac{2KT}{2n\pi} (1 - \cos n\pi)$$

$$E = -\int_{\frac{4}{6}T}^T K \sin\left(\frac{2n\pi}{T}t\right) dt = \frac{KT}{2n\pi} (1 - \cos \frac{4n\pi}{3})$$

$$F = \int_{\frac{5}{6}T}^T K \sin\left(\frac{2n\pi}{T}t\right) dt = -\frac{KT}{2n\pi} (1 - \cos \frac{5n\pi}{3})$$

$$G = \int_T^T K \sin\left(\frac{2n\pi}{T}t\right) dt = 0$$

$$b_n = \frac{2}{T} \cdot \frac{T}{2n\pi} \left[-K(1 - \cos \frac{n\pi}{3}) + K(1 - \cos \frac{2n\pi}{3}) + 2K(1 - \cos n\pi) \right.$$

$$+ K(1 - \cos \frac{4n\pi}{3}) - K(1 - \cos \frac{5n\pi}{3}) \left. \right] = \frac{1}{n\pi} [(-K+K+2K+K-K)$$

$$+ K \cos \frac{n\pi}{3} - K \cos \frac{2n\pi}{3} - 2K \cos n\pi - K \cos \frac{4n\pi}{3} + K \cos \frac{5n\pi}{3}]$$

$$b_n = \frac{1}{n\pi} \left[2K(1 - \cos n\pi) + K \left(\cos \frac{n\pi}{3} + \cos \frac{5n\pi}{3} \right) - \left\{ \cos \frac{4n\pi}{3} + \cos \frac{2n\pi}{3} \right\} \right]$$

Using the identity:

$$\cos A + \cos B = 2 \cos \left(\frac{A+B}{2} \right) \cos \left(\frac{A-B}{2} \right)$$

$$\cos \frac{n\pi}{3} + \cos \frac{5n\pi}{3} = 2 \cos n\pi \cdot \cos \frac{2n\pi}{3}$$

and

$$\cos \frac{4n\pi}{3} + \cos \frac{2n\pi}{3} = 2 \cos n\pi \cdot \cos \frac{n\pi}{3}$$

then

$$b_n = \frac{1}{n\pi} \left[2K(1 - \cos n\pi) + K \left(2 \cos n\pi \cdot \cos \frac{2n\pi}{3} - 2 \cos n\pi \cdot \cos \frac{n\pi}{3} \right) \right] = \frac{1}{n\pi} \left[2K(1 - \cos n\pi) + 2K \cos n\pi \left(\cos \frac{2n\pi}{3} - \cos \frac{n\pi}{3} \right) \right]$$

Using the identity:

$$\cos A - \cos B = -2 \sin \left(\frac{A+B}{2} \right) \sin \left(\frac{A-B}{2} \right)$$

The above expression for b_n can be further simplified:

$$b_n = \frac{1}{n\pi} \left[2K(1 - \cos n\pi) + 4K \cos n\pi \sin \frac{n\pi}{2} \sin \frac{n\pi}{6} \right]$$

If $n = \text{even}$ $\text{Cos } n\pi = 1$

$b_n = 0$ if $n = \text{even}$.

$\text{Sin } \frac{n\pi}{2} = 0$

If $n = \text{a multiple of 3, i.e., } n = 6, 12, 18 \dots$ since it

also even $b_n = 0$

If $n = 3, 9, 15 \dots$ $\text{Cos}(n\pi) = -1$

$\text{Sin}(\frac{n\pi}{2}) = +1$ and $\text{Sin}(\frac{n\pi}{6}) = +1$

However, if $\text{Sin}\frac{n\pi}{2} = +1$ then $\text{Sin}\frac{n\pi}{6} = -1$

and if $\text{Sin}\frac{n\pi}{2} = -1$ then $\text{Sin}\frac{n\pi}{6} = +1$

if $n = 3, 9, 15, \dots$ then $b_n = 0$.

The Fourier series expansion of the function $v(t)$ has only the following terms:

$n = 1, 5, 7, 11, 13, 17, 19, \dots$

and $v(t) = b_1 \text{Sin}t + b_5 \text{Sin}5t + b_7 \text{Sin}7t + b_{11} \text{Sin}11t + \dots$

where $b_n = \frac{1}{n\pi} [2K(1 - \text{Cos}n\pi) + 4K\text{Cos}n\pi \cdot \text{Sin}\frac{n\pi}{2} \cdot \text{Sin}\frac{n\pi}{6}]$

and K is the step voltage.

APPENDIX 5

COST EVALUATION

The components used in the experiment and their costs are as follows:

1.	5x(2x12V,15W) Power Supply Transformer	3750.-TL
2.	1x(25A,300V) Bridge	650.-
3.	2x(4027IC) Dual J-K Flip-Flop	300.-
4.	3x(4013IC) Dual Type D Flip-Flop	450.-
5.	1x(4011IC) Quad 2-Input "NAND" Gate	150.-
6.	1x(4050IC) Hex Buffers	150.-
7.	4x(3A,50V) Diod	200.-
8.	10x(1A,50V) Diod	150.-
9.	1x(BSV 57) U.J.T.	75.-
10.	2x(BC-107) Transistor	30.-
11.	1x(MC 7812) 12V Regulator	250.-
12.	5x(2200 μ F,50V) Capacitor	625.-
13.	6x(0.5 μ F,250V) Capacitor	300.-
14.	1x(250 μ F,400V) Capacitor	750.-
15.	6x(BD875) Darlington Transistor	240.-
16.	18x(BD699) Darlington Transistor	1800.-
17.	12x(10 Ω ,11W) Resistor	300.-
18.	1x(250V,6A) Single-phase Switch	250.-
19.	1x(400V,4A) Three-phase Switch	500.-
20.	1x(6A) Fuse	150.-
21.	1x(300V) Voltmeter	1500.-
22.	The box protection	3000.-
23.	The other components	300.-
	TOTAL	<u>15870.-TL</u>

APPENDIX 6

Schematic Diagram of the System

0-250 VDC

